

# ChemComm

Accepted Manuscript



This is an *Accepted Manuscript*, which has been through the Royal Society of Chemistry peer review process and has been accepted for publication.

*Accepted Manuscripts* are published online shortly after acceptance, before technical editing, formatting and proof reading. Using this free service, authors can make their results available to the community, in citable form, before we publish the edited article. We will replace this *Accepted Manuscript* with the edited and formatted *Advance Article* as soon as it is available.

You can find more information about *Accepted Manuscripts* in the [Information for Authors](#).

Please note that technical editing may introduce minor changes to the text and/or graphics, which may alter content. The journal's standard [Terms & Conditions](#) and the [Ethical guidelines](#) still apply. In no event shall the Royal Society of Chemistry be held responsible for any errors or omissions in this *Accepted Manuscript* or any consequences arising from the use of any information it contains.

## ARTICLE

## Oxamato-based coordination polymers: Recent advances in multifunctional magnetic materials

Cite this: DOI: 10.1039/x0xx00000x

Thais Grancha,<sup>a</sup> Jesús Ferrando-Soria,<sup>\*a</sup> María Castellano,<sup>a</sup> Miguel Julve,<sup>a</sup> Jorge Pasán<sup>b</sup> and Emilio Pardo<sup>\*a</sup>Received 00th January 2012,  
Accepted 00th January 2012

DOI: 10.1039/x0xx00000x

www.rsc.org/

The design and synthesis of novel examples of multifunctional magnetic materials based on the so-called coordination polymers (CPs) have become very attractive for chemists and physicists due to their potential applications in nanoscience and nanotechnology. However, their preparation is still an experimental challenge which requires a deep knowledge of coordination chemistry and large skills on organic chemistry. The recent advances in this field using a molecular-programmed approach based on rational self-assembly methods which fully exploit the versatility of the coordination chemistry of the barely explored and evergreen family of *N*-substituted aromatic oligo(oxamato) ligands are presented in this feature article. These exploratory studies have revealed a wide variety of interesting multifunctional magnetic materials such as optically-active chiral and luminescent magnets or dynamic porous magnets as candidates for chemical sensing. Our feeling, however, is that we have only scratched the surface of the topic and that there are many more exciting brand-new molecule-based materials waiting to be discovered.

### 1. Introduction

During the last two decades, the field of Molecular Magnetism has attracted a large number of research teams worldwide due to its multidisciplinary character.<sup>1,2</sup> In fact, it lies at the crossing point of several disciplines such as Chemistry (Inorganic and Organic Chemistry as well as Physical Chemistry), Physics (Solid State and Applied Physics as well as Theoretical Physics), and Materials Science. The convergence in this field by scientists with specific backgrounds in such different domains involves a fast and significant progress due to the complementarity between the knowledge that they possess and the techniques they use.

In relation with this multidisciplinary character, the addition of another physical property to the magnetic ones to build the so-called Multifunctional Magnetic Materials has recently become an outstanding area of research in the field Molecular Magnetism, opening new possibilities in molecule-based magnetic materials.<sup>3</sup> The main goal of this research is to synthesize and explore new classes of compounds that exhibit several properties of fundamental importance in nanoscience and nanotechnology.<sup>3a</sup> In so doing, Molecular Magnetism meets other fields of molecular sciences, such as Molecular Electronics and Photonics, Molecular Electrochemistry and Photochemistry, and Molecular Host-Guest Chemistry (including aspects of both molecular recognition and catalysis).

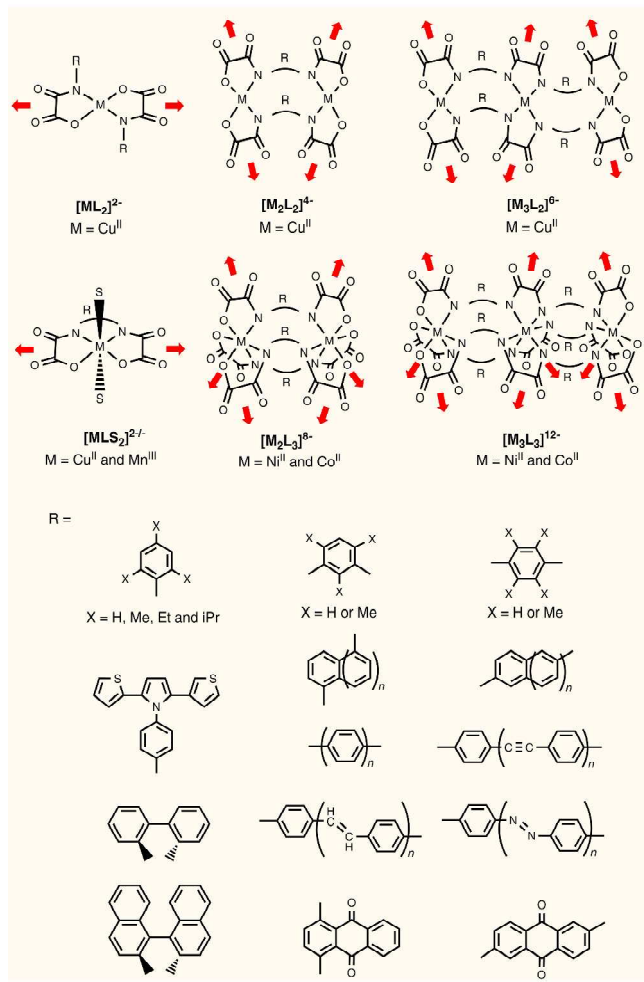
The design and synthesis of this new class of materials have largely benefited from the rapid development of a well-known branch of coordination chemistry devoted to the study of

extended metal-ligand networks, which are named coordination polymers (CPs) or Metal-Organic Frameworks (MOFs).<sup>4-8</sup> They consist of hybrid materials where metal ions or small metal clusters are linked into one-, two-, or three-dimensions (*n*D with *n* = 1–3) by a wide diversity of organic bridging ligands, giving rise to putative open-framework (porous) structures. Since the seminal work by Hoskins and Robson<sup>5</sup> and others<sup>6,7</sup> on the chemistry and magnetic properties of CPs, the interest in this field has rapidly grown over the past years following the O’Keeffe and Yaghi’s pioneering work on the sorption properties of MOFs.<sup>8</sup>

The design and synthesis of multifunctional magnetic coordination polymers (MMCPs) showing at least one physical property in addition to the magnetic ones, are formidable tasks which require a deep knowledge of both coordination chemistry and organic chemistry. On the one hand, proper choices of the organic linkers and metal ions are required in order to build CPs of variable dimensionality with interesting and predictable structural topologies and magnetic properties. On the other hand, the introduction of an additional physical property can be achieved, either by functionalizing the organic bridging ligand and/or by inserting a specific organic guest molecule into the channels of the open-framework, its properties being incorporated to the resulting hybrid inorganic-organic material (Scheme 1).

When multifunctionality arises from the presence of guest molecules present in the voids of the CPs, is more than evident that porosity is required. However, the combination of porosity and long-range magnetic ordering in the same material is an

intellectual challenge. In general, porosity requires bridging ligands with long organic spacers connecting the individual metal ions or the polymeric units that lead to an open-framework structure.<sup>8</sup> However, the long organic spacers do not facilitate the magnetic interactions between the distant metal centres. This apparent paradox to which synthetic chemists working in the field of MMCPs are faced, accounts for the small number of reports on porous magnets based on CPs.<sup>9</sup>



**Scheme 1** Molecular libraries of oligonuclear aromatic oxamate complexes used as metalloligands (S stands for labile solvent molecules). The red arrows represent the free coordination sites to build the CPs.

## 2. Molecular-programmed approach to heterobimetallic $nD$ ( $n = 1-3$ ) CPs

Coordination chemistry offers the basic tools to build MMCPs.<sup>10,11</sup> Two main different strategies can be chosen in this respect: (i) the largely spread, serendipitous self-assembly methods (often employing hydro(solvo)thermal reaction conditions),<sup>12</sup> and (ii) the use of the so-called “complex-as-ligand” strategy, where a preformed complex acts as a ligand (metalloligand) toward fully solvated paramagnetic metal ions. The second rational approach shows clear advantages against the first one. These molecular-programmed methods consist of

using a stable preformed metal complex with additional coordination sites, which can coordinate free metal ions (or coordinatively-unsaturated metal complexes) under “soft” conditions. They constitute one of the most efficient ways to gain control on the net dimensionality and topology of the CPs, allowing thus an step further to get the desired properties in a given material. However, a total control of the final architecture and properties is still exceedingly difficult in spite of these clear advantages because of the subtle factors that may affect the assembly process of metalloligands and metal ions/preformed complexes.

Two representative examples of the richness of this metalloligand design strategy are represented by the use of cyanide- and oxalate-bearing mononuclear precursors such as  $[M^{III}(CN)_6]^{3-}$  and  $[M^{III}(C_2O_4)_3]^{3-}$  ( $M = Cr$  or  $Fe$ ) as ligands towards different divalent metal ions.<sup>10,11</sup> So, the host-guest chemistry and sorption properties of the well-known families of bimetallic cyanide (Prussian blue)<sup>10</sup> and oxalato<sup>11</sup> magnets have been extensively explored affording a large variety of examples of MMCPs when incorporating guest molecules with additional properties of interest (v.g., chirality, electrical and protonic conductivity, non-linear optics, photomagnetism).<sup>10,11</sup>

Another family of related metalloligands concerns the oligonuclear complexes with *N*-substituted aromatic oligo(oxamate) ligands, as depicted in Scheme 1. They have received a comparatively less attention in spite of their potentially unique opportunities to design novel multifunctional magnetic materials that they offer.<sup>13</sup> The main advantages provided by that this type of ligands envisaging the construction of MMCPs are highlighted here:

- Firstly, the *N,O*-oxamato donor group show a great coordination affinity toward divalent first-row transition metal ions ( $M = Cu^{II}$ ,  $Ni^{II}$  and  $Co^{II}$ ) with a high stability in solution of the resulting oligonuclear complexes, from mono-, to di-, and trinuclear species (Scheme 1, top), the substitution by other divalent ions being thus precluded. This allows the formation in solution (and further isolation) of very stable and robust building blocks that have additional binding ability towards other divalent metal ions ( $M = Ni^{II}$ ,  $Co^{II}$ , and  $Mn^{II}$ ) through the free carbonyl oxygen atoms offering the possibility to obtain heterobimetallic CPs with a wide diversity of architectures.
- The bis(bidentate) oxamate bridge mediates strong magnetic coupling between the neighbouring metal ions in homo- and heterobimetallic compounds affording thus, interesting magnetic properties such as long-range 3D magnetic ordering<sup>14,15</sup> and tentatively Single-Molecule Magnet (SMM)<sup>16</sup> or Single-Chain Magnet (SCM)<sup>17</sup> behaviours.
- In some cases, oxamato-based magnets present anionic open-framework structures,<sup>14e,f,18</sup> instead of the more common neutral ones.<sup>14b-d</sup> The anionic nature of the networks together with the presence of large channels make these systems suitable candidates to obtain multifunctional materials. Indeed, different counteranions could be rationally introduced in their pores, affording the required additional physical property.
- Last but not least, is the fact that oxamate ligands can be easily functionalised just by choosing the appropriate amine precursor (Scheme 1, bottom), allowing thus, an alternative route to induce new functionalities in the material such as chirality, luminescence, photo- or redox-activity, pH-triggered switches for the reversible

formation of emulsions, and catalysts for environmentally friendly organic reactions.<sup>19</sup>

So, since the pioneering work of Kahn and coworkers in the late 1980s,<sup>20</sup> a wide variety of oxamato-based bimetallic compounds, both discrete zero-dimensional (0D) high-nuclearity complexes<sup>21</sup> as well as extended one- (1D),<sup>22</sup> two- (2D),<sup>14b-g</sup> or three-dimensional (3D)<sup>15</sup> coordination polymers with interesting and predictable magnetic properties have been reported. This is impressively demonstrated by the family of heterobimetallic CPs built from mononuclear copper(II) precursors containing polyalkyl-substituted *N*-phenyloxamate as ligands. Hereafter, we briefly develop our results on this topic in order to nicely illustrate some of the aforementioned advantages of the metalloligand strategy towards oxamate-based magnetic coordination polymers.

## 2.1 Single-chain magnetic behaviour in linear 1D CPs

The observation of slow magnetic relaxation and hysteresis effects in a cobalt(II)-nitronyl nitroxide radical chain<sup>23a</sup> which was not associated to a 3D ordering but having a purely 1D origin, the so-called Single-Chain Magnet behaviour (SCM)<sup>23</sup> has provided an experimental confirmation of the Glaubers' prediction<sup>24</sup> and opened exciting new perspectives for storing information in low-dimensional magnetic materials (see discussion below).

In order to prepare novel examples of SCMs, we designed an alternative synthetic strategy based on the use of sterically hindered dianionic oxamato-containing copper(II) mononuclear complexes (Scheme 1) as bis(bidentate) metalloligands (instead of the organic nitronyl nitroxide radicals) towards Co<sup>II</sup> ions in aqueous solution. This approach resulted in an oxamato-bridged heterobimetallic cobalt(II)-copper(II) linear chain of formula [CoCu(2,4,6-Me<sub>3</sub>pa)<sub>2</sub>(H<sub>2</sub>O)<sub>2</sub>]<sub>n</sub> · 4nH<sub>2</sub>O, where 2,4,6-Me<sub>3</sub>pa = *N*-2,4,6-trimethylphenyloxamate (Fig. 1).<sup>17</sup> The combination in this 1D CP of highly anisotropic, *trans*-diaquabis(chelated) octahedral high-spin Co<sup>II</sup> ions with the presence of the bulky trimethyl-substituted phenyl groups from the [Cu<sup>II</sup>(2,4,6-Me<sub>3</sub>pa)<sub>2</sub>]<sup>2-</sup> precursor afford an Ising-type chain magnetic anisotropy and a large separations between adjacent chains. The minimisation of the interchain interactions in this Ising chain is most likely responsible for the observation of the SCM behaviour at a low blocking temperature (*T*<sub>B</sub> ≈ 2 K) for the first time in a bimetallic ferrimagnetic chain.

## 2.2 Long-range magnetic ordering in 2D hexagonal and 3D decagonal CPs

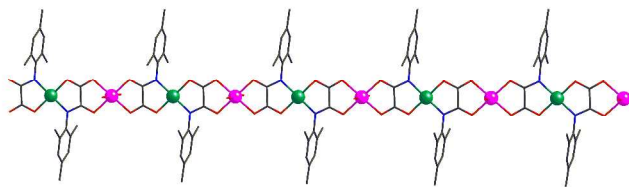


**Fig. 1** View of a fragment of the chain [CoCu(2,4,6-Me<sub>3</sub>pa)<sub>2</sub>(H<sub>2</sub>O)<sub>2</sub>]<sub>n</sub> · 4nH<sub>2</sub>O showing the *trans* arrangement of the bulky trimethyl-substituted phenyl groups. The Cu<sup>II</sup> and Co<sup>II</sup> atoms are depicted as green and purple spheres, respectively.

By using the related pair of dianionic mononuclear copper(II) complexes [Cu<sup>II</sup>(Me<sub>2</sub>pa)<sub>2</sub>]<sup>2-</sup> and [Cu<sup>II</sup>(Et<sub>2</sub>pa)<sub>2</sub>]<sup>2-</sup> (2,6-Me<sub>2</sub>pa = *N*-2,6-dimethylphenyloxamate and 2,6-Et<sub>2</sub>pa = *N*-2,6-diethylphenyloxamate), as bis(bidentate) metalloligands towards Mn<sup>II</sup> ions in dimethylsulphoxide (dmsO) solution, two novel oxamato-bridged heterobimetallic 2D and 3D CPs of

formulas (*n*-Bu<sub>4</sub>N)<sub>4</sub>[Mn<sub>4</sub>Cu<sub>6</sub>(2,6-Me<sub>2</sub>pa)<sub>12</sub>] · 2dmsO (2D) and (*n*-Bu<sub>4</sub>N)<sub>4</sub>[Mn<sub>4</sub>Cu<sub>6</sub>(2,6-Et<sub>2</sub>pa)<sub>12</sub>] (3D) [*n*-Bu<sub>4</sub>N<sup>+</sup> = tetra-*n*-butylammonium cation] were obtained (Fig. 2).<sup>15</sup> Upon coordination, the corresponding [Cu<sup>II</sup>L<sub>2</sub>]<sup>2-</sup> precursor (L = 2,6-Me<sub>2</sub>pa and 2,6-Et<sub>2</sub>pa) transfers the steric information of its bulky dialkyl-substituted phenyl groups in *trans* arrangement into the stereochemistries of the tris(chelated) Mn<sup>II</sup> metal centres yielding two coordination polymers of different dimensionality [2D (L = Me<sub>2</sub>pa) and 3D (L = Et<sub>2</sub>pa)] as a result of the different steric effects introduced by the methyl and ethyl substituents in the phenyl ring.

The structure of the compound (*n*-Bu<sub>4</sub>N)<sub>4</sub>[Mn<sub>4</sub>Cu<sub>6</sub>(2,6-Me<sub>2</sub>pa)<sub>12</sub>] · 2dmsO consists of anionic oxamato-bridged Mn<sup>II</sup><sub>2</sub>Cu<sup>II</sup><sub>3</sub> hexagonal layers of 6<sup>3</sup> net topology growing in the crystallographic *ab* plane (Fig. 2a). Within each bimetallic hexagonal ring, the chirality of the tris(chelated) octahedral Mn<sup>II</sup> ions follows the 'ΔΔ' sequence. Each Mn<sup>II</sup><sub>2</sub>Cu<sup>II</sup><sub>3</sub> hexagonal layer can be alternatively described as an extended parallel array of oxamato-bridged manganese(II)-copper(II) chains which are further connected by additional bis(bidentate) copper(II) precursors.

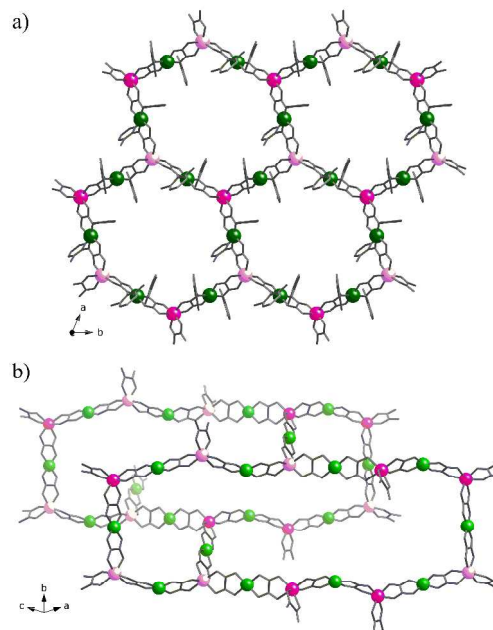


**Fig. 2** Perspective view of a fragment of (*n*-Bu<sub>4</sub>N)<sub>4</sub>[Mn<sub>4</sub>Cu<sub>6</sub>(Me<sub>2</sub>pa)<sub>12</sub>] · 2dmsO (a) and (*n*-Bu<sub>4</sub>N)<sub>4</sub>[Mn<sub>4</sub>Cu<sub>6</sub>(Et<sub>2</sub>pa)<sub>12</sub>] (b). Metal and ligand atoms are represented by balls and sticks, respectively [Cu, green; (Δ)-Mn, purple; (Λ)-Mn, pink].

On the contrary, the structure of (*n*-Bu<sub>4</sub>N)<sub>4</sub>[Mn<sub>4</sub>Cu<sub>6</sub>(Et<sub>2</sub>pa)<sub>12</sub>] is made up by an anionic oxamato-bridged Mn<sup>II</sup><sub>2</sub>Cu<sup>II</sup><sub>3</sub> 3D decagonal network with a 10<sup>3</sup>-th net topology (Fig. 2b). Within each Mn<sup>II</sup><sub>2</sub>Cu<sup>II</sup><sub>3</sub> decagonal ring, the chirality of the tris(chelated) octahedral Mn<sup>II</sup> ions follows the 'ΔΔΔ' sequence. This unprecedented situation leads to an overall achiral Mn<sup>II</sup><sub>2</sub>Cu<sup>II</sup><sub>3</sub> decagonal framework which results from the existence of two different bis(bidentate) copper(II) precursors connecting the Mn<sup>II</sup> centres of the same (Δ-Mn-Δ-Mn and Λ-Mn-Λ-Mn) and opposite (Δ-Mn-Λ-Mn) chiralities.

As expected from the different dimensionality in these compounds, their magnetic properties differ drastically. However, although both 2D and 3D CPs exhibit magnetic ordering, the values of the Curie temperature (*T*<sub>C</sub>) are quite

different. So, a long-range ferromagnetic ordering occurs in the compound  $(n\text{-Bu}_4\text{N})_4[\text{Mn}_4\text{Cu}_6(\text{Me}_2\text{pma})_{12}] \cdot 2\text{dmsO}$  which results from the weak (most likely dipolar) ferromagnetic interactions between the ferrimagnetic  $\text{Mn}^{\text{II}}_2\text{Cu}^{\text{II}}_3$  hexagonal layers at  $T_C = 10$  K. In contrast, the intrinsically three-dimensional character of the complex  $(n\text{-Bu}_4\text{N})_4[\text{Mn}_4\text{Cu}_6(\text{Et}_2\text{pma})_{12}]$  allows the observation of a long-range ferrimagnetic order of the  $\text{Mn}^{\text{II}}_2\text{Cu}^{\text{II}}_3$  decagonal net at a somewhat greater value of the critical temperature ( $T_C = 25$  K).

In summary, we have shown some previous results of oxamato-based CPs that highlight the interesting magnetic properties that these bridging ligands can afford. It deserves to be noted that additional physical properties have been rationally introduced in these systems only very recently providing the first examples of oxamato-based MMCPs.<sup>25-29</sup> Indeed, the variety of multifunctional magnetic behaviours reported in this review, ranging from optically-active chiral and luminescent magnets to porous magnets, illustrates the potential of oxamato-based heterobimetallic coordination polymers in the field of MMCPs. Let us briefly develop all these topics in the following sections by including a proposal of the main objectives and application domains for each type of oxamato-based MMCPs.

### 3. Optically-active chiral magnets

#### 3.1 Single-chain magnetic behaviour in enantiopure zigzag 1D CPs

Among the molecule-based low-dimensional magnetic materials, the aforementioned 1D coordination polymers exhibiting slow magnetic relaxation below a blocking temperature ( $T_B$ ) are particularly appealing to get MMCPs. These compounds, which are called Single Chain Magnets (SCMs)<sup>17,23</sup> by analogy to the single molecule magnets (SMMs),<sup>16,30</sup> offer the great advantage of achieving information storage at higher temperatures. In fact, SMMs have a high-spin ( $S$ ) ground state with an important Ising-type magnetic anisotropy ( $D$ ) that results in a large activation energy ( $E_a$ ) for the magnetisation reversal, given by  $E_a = |D|S^2$  (for an integer  $S$ ). In the case of SCMs, the activation energy also depends upon the intrachain magnetic coupling ( $J$ ) according to the expression  $E_a = (4|J| + |D|)S^2$ . That being so, many groups have focused their efforts on the search for SCMs instead of SMMs because of the possibility of increasing the value of  $T_B$  by enhancing the intrachain interactions and thus opening the way to future applications of molecular nanomagnets in nanoscience and nanotechnology.<sup>31</sup>

After the publication in 2001 of the first example reported by Gatteschi *et al.*,<sup>23a</sup> which still exhibits the highest blocking temperature observed so far ( $T_B \approx 15$  K), some additional examples of SCMs were published during the following years because of the possibility of storing information in these low-dimensional magnetic materials. However, from the relatively wide variety of examples of SCMs published until 2010,<sup>17,23</sup> none of them showed another physical property in addition to the magnetic one. So, for instance, the combination of slow magnetization relaxation effects (characteristic of SCMs) and optical properties (typical of chiral organic compounds) opens new exciting perspectives for storing information in the domain of MMCPs.

In a recent work,<sup>25</sup> we proposed for the first time a rational enantioselective synthetic strategy to obtain chiral heterobimetallic chains based on the use of sterically-hindered, chiral dianionic mononuclear copper(II) complexes with the enantiomerically pure (*M*)-1,1'-binaphthalene-2,2'-bis(oxamate)

[(*M*)-binaba] and (*P*)-1,1'-binaphthalene-2,2'-bis(oxamate) [(*P*)-binaba] ligands (Scheme 1). This pair of *M* and *P* helical-type mononuclear copper(II) enantiomers,  $[\text{Cu}[(\text{M}/\text{P})\text{-binaba}]]^{2-}$  (Scheme 1a), acting as bis(bidentate) metalloligands towards doubly *cis*-solvated ( $S = \text{dmsO}$  and  $\text{dmf}$ ), divalent transition metal cations like manganese(II) and cobalt(II), transfer their chiral information to the stereochemistry of the octahedral  $\text{M}^{\text{II}}$  metal centres (*A* and  $\Delta$  propeller-type enantiomers) in a controlled manner and consequently, a predetermination of the absolute configuration of the final  $\text{Cu}^{\text{II}}\text{M}^{\text{II}}$  chain could be achieved.<sup>32</sup> Indeed, enantiopure chiral chains of general formula  $\text{MCuL}(\text{S})_m(\text{H}_2\text{O})_n \cdot a\text{S} \cdot b\text{H}_2\text{O}$  made up by the repetition of the corresponding neutral chiral (*M*)- $\text{Cu}^{\text{II}}(\text{A})\text{-M}^{\text{II}}$  and (*P*)- $\text{Cu}^{\text{II}}(\Delta)\text{-M}^{\text{II}}$  units (Fig. 3a and b) were obtained when using the mononuclear (*M*)- and (*P*)-copper(II)-binaba complexes, respectively. On the contrary, when using the racemic mononuclear copper(II)-binaba complex, an achiral zigzag  $\text{Cu}^{\text{II}}\text{M}^{\text{II}}$  chain was obtained, consisting of alternating (*M*)- $\text{Cu}^{\text{II}}(\text{A})\text{-M}^{\text{II}}$ -(*P*)- $\text{Cu}^{\text{II}}(\Delta)\text{-M}^{\text{II}}$  units (Fig. 3c). Therefore, this molecular-programmed approach allowed the rational preparation of enantiopure chiral and racemic achiral, oxamato-bridged heterobimetallic chains. CD spectra of the heterobimetallic chain compounds confirmed the absolute configuration of the chiral metal centres in each case, by the occurrence of large, either negative or positive Cotton effects for the enantiopure chains of opposite chirality and conversely, by their absence in the racemic achiral ones (Fig. 4a).

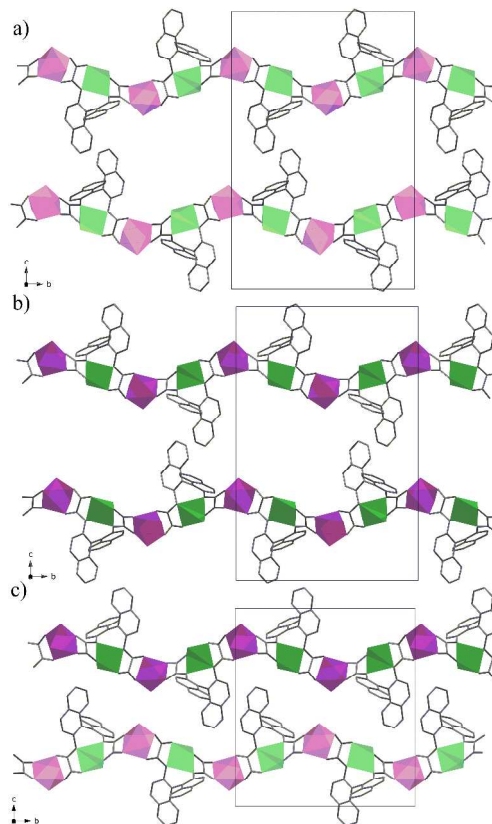


**Fig. 3** Views of the crystal packing of the chains of  $[(\text{M})\text{-Cu}^{\text{II}}(\text{A})\text{-Mn}^{\text{II}}]_n$  (a),  $(\text{P})\text{-Cu}^{\text{II}}(\Delta)\text{-Mn}^{\text{II}}]_n$  (b) and the racemic compound (c) in the crystallographic  $bc$  plane. Hydrogen atoms and crystallization solvent molecules have been omitted for clarity. The (*A*)- $\text{Mn}^{\text{II}}$  and ( $\Delta$ )- $\text{Mn}^{\text{II}}$  atoms are depicted as pale and dark purple polyhedra respectively, whereas the (*M*)- $\text{Cu}^{\text{II}}$  and (*P*)- $\text{Cu}^{\text{II}}$  atoms are drawn as pale and dark green polyhedra.

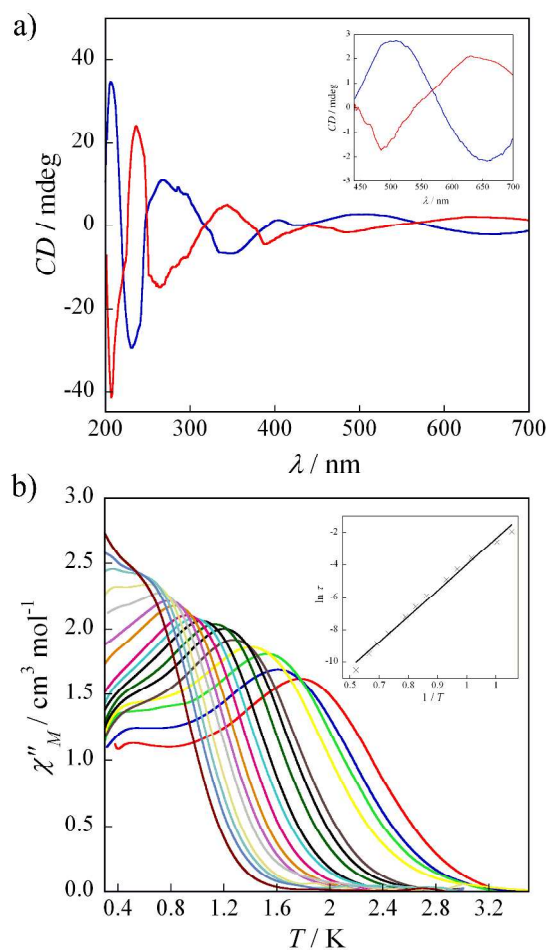


**Fig. 4** (a) Solid CD spectra of the  $[(M)\text{-Cu}^{\text{II}}\text{-(A)-Co}^{\text{II}}]_n$  (blue) and  $[(P)\text{-Cu}^{\text{II}}\text{-(A)-M}^{\text{II}}]_n$  (red) chains. The inset shows the CD spectra in the visible region. (b) Temperature dependence of the out-of-phase magnetic susceptibility of the  $[(M)\text{-Cu}^{\text{II}}\text{-(A)-Co}^{\text{II}}]_n$  chain under zero applied static field at different frequencies (0.021–5700 Hz) of the  $\pm 1$  G oscillating field. The inset shows the Arrhenius plot.

Indeed, the enantiopure  $\text{Co}^{\text{II}}\text{Cu}^{\text{II}}$  chains showed slow magnetic relaxation effects that are typical of SCMs, as revealed by the presence of a frequency-dependent peak around  $T_B = 2.0$  K in the out-of-phase alternating current (ac) magnetic susceptibility measurements at very low temperatures (Fig. 4b). Certain structural (steric) as well as electronic (magnetic anisotropy) requirements on both the organic ligand and the divalent metal ion respectively, must be fulfilled in order to observe this phenomenon. So, the bulky 1,1'-binaphthalene organic spacer of the  $(M/P)\text{-rac}$ -binaba ligand allows a good separation between neighbouring chains while the oxamato bridge transmit efficiently the antiferromagnetic interaction between the copper(II) and cobalt(II) ions. Moreover, the large local magnetic anisotropy of the orbitally degenerate octahedral high-spin  $\text{Co}^{\text{II}}$  ions is ultimately responsible for the occurrence of a large Ising-type magnetic anisotropy along the chain. In the case of the racemic  $\text{Co}^{\text{II}}\text{Cu}^{\text{II}}$  analogue, the interchain magnetic interactions preclude the observation of the SCM behaviour.

Hence, slow relaxation of the magnetisation was observed in the chiral  $\text{Co}^{\text{II}}\text{Cu}^{\text{II}}$  derivatives for the first time in enantiopure magnetic chain compounds, constituting thus the first examples of a new class of MMCPs, referred to as chiral single chain magnets (CSCMs). Interestingly, the presence of an additional

frequency-independent peak below the blocking temperature suggests the occurrence of a long-range 3D antiferromagnetic order of the chains, which are not perfectly isolated in the crystal lattice (Fig. 4b). However, the greater magnitude of the interchain magnetic interactions precludes the observation of slow magnetic relaxation effects in the case of the racemic  $\text{Co}^{\text{II}}\text{Cu}^{\text{II}}$  chain. The large magnetic moment due to the CSCM behaviour of the one-dimensional array of magnetic ions which are also the chiral centres ensures a strong coupling effect between the two physical properties, opening thus excellent perspectives to study for the first time the magnetochiral dichroism effect (see discussion below) in enantiopure 1D compounds with a higher  $T_B$ .<sup>33</sup>

### 3.2 Chiral cation-templated solid-state aggregation of enantiopure 1D double-helical CPs

Optically active, chiral magnets have given rise to interesting magneto-chiral dichroic effects<sup>11c,33</sup> because of the coexistence of asymmetry and magnetic ordering. In addition, the presence of non-centrosymmetric space groups can lead to interesting ferroelectric properties<sup>11b,34</sup> as well as non-linear optics (NLO).<sup>35</sup> However, it is not always possible to obtain the desired chiral magnets when using chiral templating cations because of the problems related to the fact that a chiral induction from the cation to the stereochemistries of the metal ions from the covalent framework is not always guaranteed. By the way, all the efforts devoted to the synthesis of chiral oxamato-based 3D CPs had been unsuccessful until very recently.

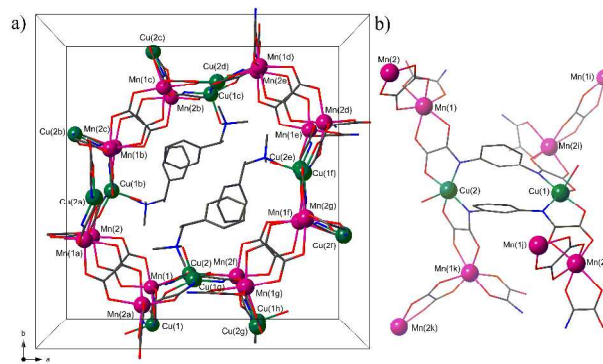


**Fig. 5** (a) Perspective view of the unit cell of  $[(S)\text{-(1-PhEt)Me}_3\text{N}]_2[\text{Mn}_2(\text{ox})\text{Cu}_2(\text{mpba})_2(\text{H}_2\text{O})_2] \cdot 3\text{H}_2\text{O}$  with the metal atom labelling showing the filling of the octagonal pores by the counteranions. (b) View of a fragment of  $[(S)\text{-(1-PhEt)Me}_3\text{N}]_2[\text{Mn}_2(\text{ox})\text{Cu}_2(\text{mpba})_2(\text{H}_2\text{O})_2] \cdot 3\text{H}_2\text{O}$  with the numbering of the metal ions.

In that sense, the use of the anionic double-stranded dicopper(II) complex,  $[\text{Cu}_2(\text{mpba})_2]^{4-}$  [ $\text{mpba} = N,N'\text{-1,3-phenylenebis(oxamate)}$ ] (Scheme 1b), as tetrakis(bidentate) metalloligand towards bis(chelated)  $\text{M}^{2+}$  ions ( $\text{M} = \text{Mn}$  and  $\text{Co}$ ) yields neutral achiral oxamato-based 1D or 2D CPs with either “ladderlike” or “brickwall” topologies<sup>14b-g</sup> respectively, even in the presence of chiral templating cations.

In order to achieve the first oxamato-based chiral 3D magnet, we explored a new rational synthetic strategy based on the use of the templating chiral  $(S)$ -trimethyl(1-phenylethyl)ammonium cation,  $[(S)\text{-(1-PhEt)Me}_3\text{N}^+]$ , together with the oxalate dianion during the self-assembly process of  $[\text{Cu}^{\text{II}}(\text{mpba})_2]^{4-}$  with  $\text{Mn}^{2+}$  ions. This reaction led to a novel chiral manganese(II)-copper(II) 3D compound of formula  $[(S)\text{-(1-PhEt)Me}_3\text{N}]_2[\text{Mn}_2(\text{C}_2\text{O}_4)\text{Cu}_2(\text{mpba})_2(\text{H}_2\text{O})_2] \cdot 3\text{H}_2\text{O}$  (Fig.

5).<sup>26</sup> Its crystal structure consists of a mixed oxalato/oxamato-based heterobimetallic chiral 3D open-framework with small square and large octagonal pores of approximate dimensions  $0.70 \times 0.70$  nm and  $1.75 \times 1.75$  nm respectively, which are occupied by the  $(S)$ -(1-PhEt)Me<sub>3</sub>N<sup>+</sup> counteranions and crystallisation water molecules (Fig. 5). Interestingly, the anionic 3D network possesses a unprecedented binodal 3,4-connected  $[(4.6.8)_2(4^2.6.8^2.10)]$ -net topology when considering the dicopper(II) units and the manganese(II) ions as four- and three-fold nodes, respectively (Fig. 6).

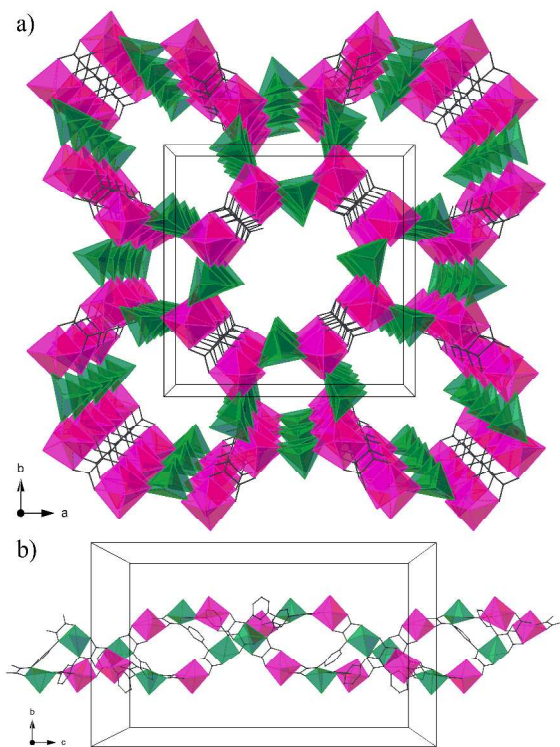


**Fig. 6** (a) Perspective view of the anionic 3D network of  $[(S)$ -(1-PhEt)Me<sub>3</sub>N]<sub>2</sub>[Mn<sub>2</sub>(ox)Cu<sub>2</sub>(mpba)<sub>2</sub>(H<sub>2</sub>O)<sub>2</sub>] $\cdot$  3H<sub>2</sub>O along the crystallographic  $c$  axis. (b) View of a fragment of the double helical chain motif of  $[(S)$ -(1-PhEt)Me<sub>3</sub>N]<sub>2</sub>[Mn<sub>2</sub>(ox)Cu<sub>2</sub>(mpba)<sub>2</sub>(H<sub>2</sub>O)<sub>2</sub>] $\cdot$  3H<sub>2</sub>O along the crystallographic  $c$  axis. Metal and ligand atoms are represented by polyhedra and sticks, respectively (Cu, green; Mn, purple). Hydrogen atoms, counteranions and crystallization water molecules are omitted for clarity.

The anionic 3D network of the compound  $[(S)$ -(1-PhEt)Me<sub>3</sub>N]<sub>2</sub>[Mn<sub>2</sub>(ox)Cu<sub>2</sub>(mpba)<sub>2</sub>(H<sub>2</sub>O)<sub>2</sub>] $\cdot$  3H<sub>2</sub>O can be alternatively described as an extended array of neutral oxamato-bridged manganese(II)-copper(II) double helical chains running parallel to the crystallographic  $c$  axis, which are further interconnected by the oxalate group acting as a bis-bidentate linker between two manganese(II) ions of the neighbouring double helical chains (Fig. 6a). Within each double helix, the pair of Mn<sup>II</sup>Cu<sup>II</sup> chains related by a 4<sub>1</sub> axis are interconnected through the two  $m$ -phenylenediamidate bridges between the Cu<sup>II</sup> ions, which would act as “bridge tights” (Fig. 6b). The shape of these right-handed double-stranded helices is reminiscent of that found for the well-known A-DNA double helix, where the two  $m$ -phenylene spacers stack each other in a similar way to that observed for the nucleobases in the DNA double helix. Most likely, the weak intermolecular (van der Waals and/or electrostatic) interactions between the  $(S)$ -(1-PhEt)Me<sub>3</sub>N<sup>+</sup> guest cations and the anionic 3D host

network (Fig. 5a) account for the right-handed chirality of the constituting double helices, so that the use of  $(R)$ -(1-PhEt)Me<sub>3</sub>N<sup>+</sup> guest cations would lead to an identical anionic 3D host network but having double helices of left-handed chirality. These chiral cation templating effects would be also responsible for the formation of chiral double helices instead of the aforementioned achiral ladders<sup>14b-g</sup> as constituting units of the anionic 3D network.

The direct current (dc) magnetic susceptibility measurements of  $[(S)$ -(1-PhEt)Me<sub>3</sub>N]<sub>2</sub>[Mn<sub>2</sub>(ox)Cu<sub>2</sub>(mpba)<sub>2</sub>(H<sub>2</sub>O)<sub>2</sub>] $\cdot$  3H<sub>2</sub>O revealed a typical 1D ferrimagnetic behaviour at high temperatures resulting from the strong antiferromagnetic intrachain interactions between the Mn<sup>II</sup> and Cu<sup>II</sup> ions through the oxamato bridge within the double helical chain. At low temperatures, however, the moderately strong antiferromagnetic interchain interaction between the Mn<sup>II</sup> ions of neighbouring double helical chains through the oxalate bridge dominates over the weak ferromagnetic intrachain interactions between the Cu<sup>II</sup> ions through the double  $m$ -phenylene bridge within the double helical chains. Nevertheless, no evidence of long-range 3D magnetic ordering above 2.0 K was found from the low-temperature heat capacity measurements.

## 4. Dynamic Porous magnets

### 4.1 Multifunctional switching in a 3D square/octagonal coordination polymer with sponge-like dynamic behaviour

The concept of “molecular magnetic sponges”, referring to the exotic sponge-like behaviour of certain molecule-based materials that undergo a dramatic change of their magnetic properties upon reversible dehydration/rehydration processes, was introduced for the first time in 1999 by Olivier Kahn.<sup>36a</sup> This was exemplified by the compound of formula  $[\text{CoCu}(\text{obbz})(\text{H}_2\text{O})_4] \cdot 2\text{H}_2\text{O}$ <sup>36b</sup> [obbz = oxamidato- $N,N'$ -bis(2-benzoate)], which is able to reversibly release and uptake five water molecules, switching from a non-magnetic ground state in the hydrated phase to as a hard magnet in the dehydrated one.

In a recent work, we obtained a novel oxamato-based manganese(II)-copper(II) 3D CP of formula  $[\text{Na}(\text{H}_2\text{O})_4]_4\{\text{Mn}_4[\text{Cu}_2(\text{mpba})_2(\text{H}_2\text{O})_4]_3\} \cdot 56.5\text{H}_2\text{O}$  by the reaction of  $\text{Na}_4[\text{Cu}_2(\text{mpba})_2] \cdot 10\text{H}_2\text{O}$  and  $\text{Mn}(\text{NO}_3)_2 \cdot 4\text{H}_2\text{O}$  in water.<sup>27</sup> This new example of MMCP exhibits a reversible solvent-induced optical, mechanical, and magnetic switching between a high- and a low-temperature ferromagnetic ordered phase upon loss of all the water molecules to give the amorphous dehydrated derivative of formula  $\text{Na}_4[\text{Mn}_4\text{Cu}_6(\text{mpba})_6]$ . Under identical conditions, however, the reaction of  $\text{Na}_4[\text{Cu}_2(\text{mpba})_2] \cdot 10\text{H}_2\text{O}$  and  $\text{Co}(\text{NO}_3)_2 \cdot 4\text{H}_2\text{O}$  in water gave the oxamato-based cobalt(II)-copper(II) 2D CP of formula  $\text{Co}_2\text{Cu}_2(\text{mpba})_2(\text{H}_2\text{O})_4$ , which exhibits a metamagnetic behaviour with a field-induced transition from an antiferro- to a ferromagnetic ordered state.<sup>14b</sup>

The anionic 3D network of  $[\text{Na}(\text{H}_2\text{O})_4]_4\{\text{Mn}_4[\text{Cu}_2(\text{mpba})_2(\text{H}_2\text{O})_4]_3\} \cdot 56.5\text{H}_2\text{O}$  can be best described as an extended parallel array of oxamato-bridged manganese(II)-copper(II) layers with a mixed square/octagonal ( $4\cdot 8^2$ ) net topology, which are further interconnected through two  $m$ -phenylene spacers between the copper(II) ions, acting as pillars in an alternately up and down disposition, to give a trinodal (3,4,4) net

with a  $(6^3)(6^4 \cdot 8^2)(6^4 \cdot 8 \cdot 10)$  topology (Fig. 7a). Overall, this situation leads to a bimodal pore size distribution, with small square and large octagonal pores of approximate dimensions  $1.2 \times 1.2$  nm and  $2.1 \times 3.0$  nm respectively, which are occupied by the coordinated  $\text{Na}^+$  counteranions and a large amount of both coordinated and hydrogen-bonded water molecules (Fig. 7b). The estimated empty volume without the crystallization water molecules is  $13580 \text{ \AA}^3$ , a value which represents up to *ca.* 70% of potential void per unit cell volume [ $V = 19746(6) \text{ \AA}^3$ ].

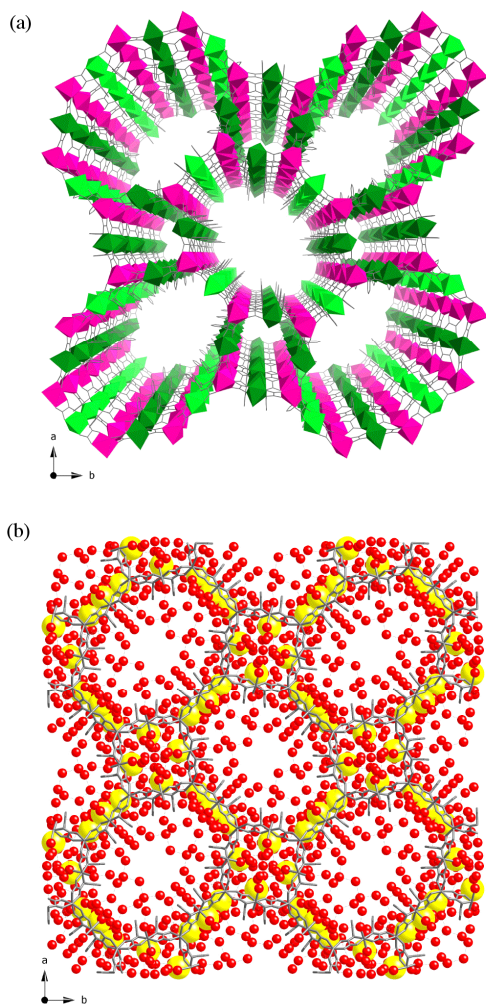


**Fig. 7** (a) Perspective view of  $\text{Na}_4[\text{Mn}_4\text{Cu}_6(\text{mpba})_6(\text{H}_2\text{O})_{12}] \cdot 72.65 \text{ H}_2\text{O}$  along the crystallographic *c* axis. Cu and Mn atoms are represented by green and purple octahedra, respectively. (b) Projection view of the crystal packing along the crystallographic *c* axis showing the filling of the small square and large octagonal pores of the open-framework structure by solvated sodium counteranions (yellow spheres) as well as coordinated and free water molecules (red spheres).

A crystalline-to-amorphous-like transition from  $[\text{Na}(\text{H}_2\text{O})_4]_4\{\text{Mn}_4[\text{Cu}_2(\text{mpba})_2(\text{H}_2\text{O})_4]_3\} \cdot 56.5\text{H}_2\text{O}$  to  $\text{Na}_4[\text{Mn}_4\text{Cu}_6(\text{mpba})_6]$  occurs upon removal of all crystallisation and weakly coordinated water molecules from by heating at  $150 \text{ }^\circ\text{C}$ . This process is accompanied by a colour change of the crystals from bright to dark green and by a significant crystal contraction with an estimated change of volume of *ca.* 45% (Fig. 8a). This transformation is reversible as evidenced by the recovery of the

original volume and bright green colour of the crystals under rehydration. This dynamic behaviour in flexible MOFs is a well-established phenomenon since the pioneering work by Kitagawa and Férey.<sup>37,38</sup> So, for instance, the well-known family of iron(III) or chromium(III) frameworks with aliphatic and aromatic dicarboxylates as organic bridging ligands (MIL-88A–D) undergoes a volume change of up to *ca.* 300% upon desolvation.<sup>39</sup>

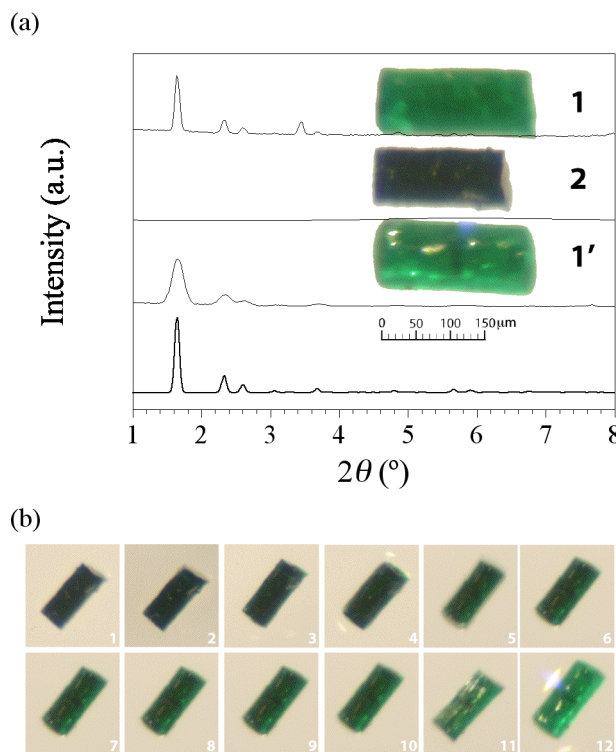


**Fig. 8** (a) XRPD patterns of the hydrated (1), dehydrated (2), and rehydrated species (1') at  $25 \text{ }^\circ\text{C}$  along with the corresponding single-crystal optical microscopy images. The bold line corresponds to the calculated XRPD pattern of 1. (b) Optical microscopy images of one single crystal of 2 taken every minute after immersion into water showing the colour and volume changes that accompany the rehydration process.

Indeed, the combination of reversible optical and mechanical switching behaviours in this compound is a rare phenomenon, which was earlier observed in a 2D honeycomb copper(II) framework with polychlorinated triphenylmethyl tricarboxylate radicals as paramagnetic organic bridging ligands (MOROF-1).<sup>40</sup> The simultaneous and gradual colour change and volume expansion of the crystal during the rehydration process have been followed by optical microscopy (Fig. 8b). These solvent-induced breathing-type dynamic effects suggest a reversible collapse/reconstruction of the open-framework structure after water removal and retrieval from the pores, in agreement with the gas sorption studies. In this sense, the  $\text{CO}_2$  and  $\text{N}_2$  adsorption/desorption isotherms show almost no porosity, suggesting the collapse of the pore system upon dehydration.<sup>41</sup> On the other hand, the reversible colour change from bright to dark green is likely attributed to the variation in the copper(II) surrounding from six- ( $\text{CuN}_2\text{O}_2\text{Ow}_2$ ) to four-coordination ( $\text{CuN}_2\text{O}_2$ ) upon removal of the two weakly bound axial water

molecules, while the six-coordinate manganese(II) environment remains unchanged ( $\text{MnO}_6$ ).

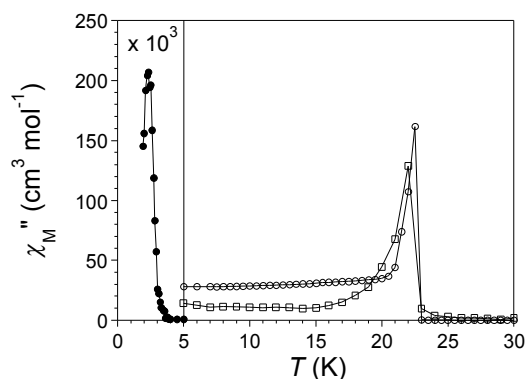


**Fig. 9** Temperature dependence of the alternating current (ac) out-of-phase ( $\chi''$ ) magnetic susceptibility of the hydrated (O), dehydrated (●) and rehydrated (□) species.

In addition to these solvent-triggered mechanical and optical changes, a drastic variation of the long-range ferromagnetic ordering temperature was also observed as a function of the water contents, as

expected for a magnetic sponge. The alternating current (ac) magnetic susceptibility measurements confirm the occurrence of a long-range 3D ferromagnetic ordering at a critical temperature ( $T_c$ ) of 22.5 K for the hydrated phase, this temperature being shifted to 2.3 K for the dehydrated derivative (Fig. 9). Moreover, a complete recovering of the long-range 3D ferromagnetic ordering is observed when rehydrating, confirming thus the reversible nature of the dehydration/rehydration processes. The drastic variation of the long-range ferromagnetic ordering temperature as a function of the water contents in this novel class of oxamato-based porous magnets with open metal sites and pore spaces offers fascinating possibilities in chemical sensing of small guest molecules (such as other coordinating solvents and gases), as we will show hereafter.

#### 4.2 Selective gas and vapour sorption and magnetic sensing by a 3D square/octagonal coordination polymer

Among the variety of MMOPs, porous magnets – where the sorption properties coexist with a long-range magnetic ordering – have become one of the most challenging research fields for a great number of chemists, physicists, and materials scientists. The main goal with these materials is the modulation of the magnetic properties of the host open-framework by the inclusion of selected guests such as solvents or gases through

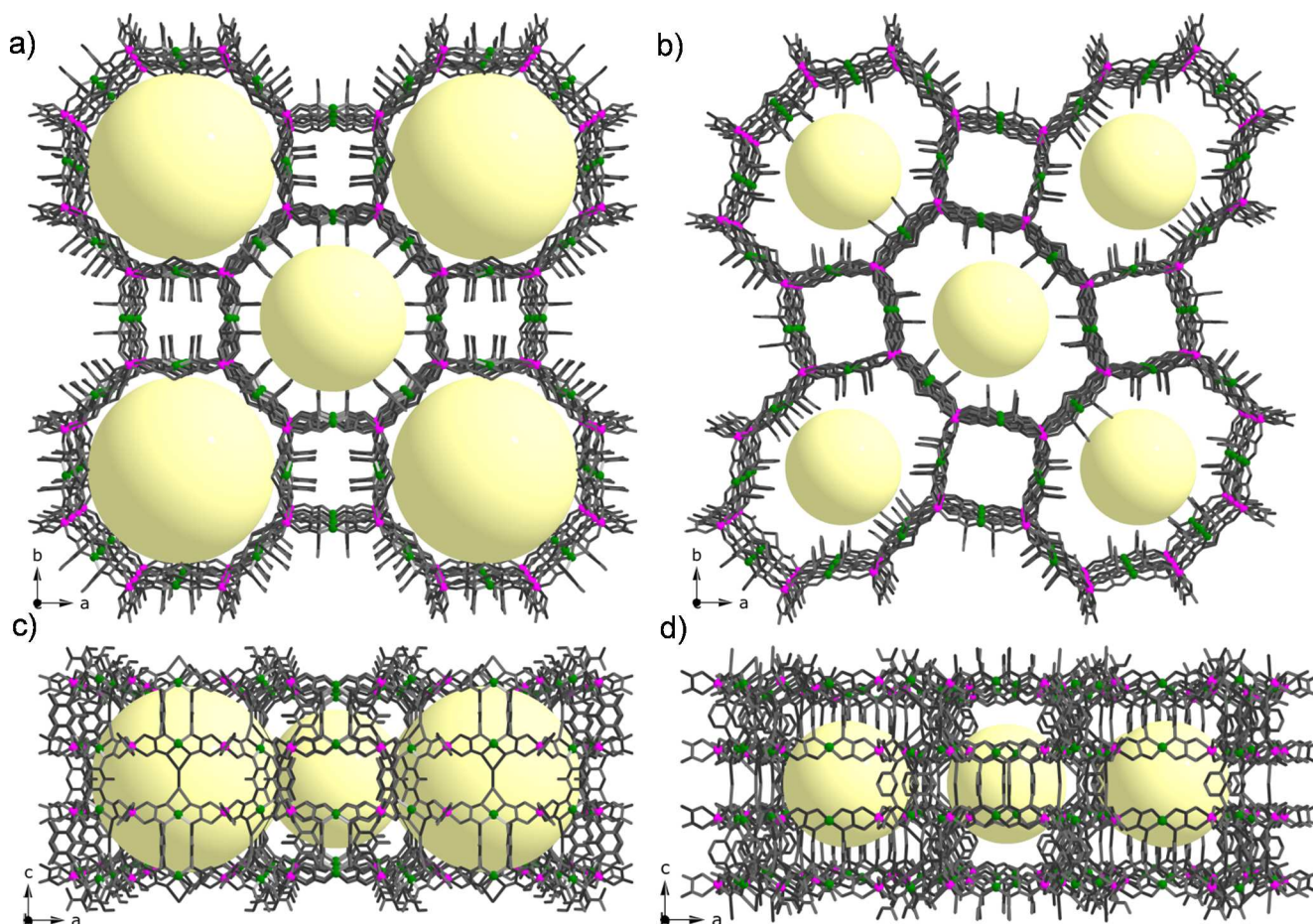


**Fig. 10** Projection views of the crystal packing of  $[\text{Na}(\text{H}_2\text{O})_{3.25}]_4\{\text{Mn}_4[\text{Cu}_2(\text{Me}_3\text{mpba})_2(\text{H}_2\text{O})_{3.33}]_3\} \cdot 37 \text{H}_2\text{O}$  (a and c) and  $[\text{Na}(\text{H}_2\text{O})_4]_4\{\text{Mn}_4[\text{Cu}_2(\text{mpba})_2(\text{H}_2\text{O})_4]_3\} \cdot 56.5 \text{H}_2\text{O}$  (b and d) along the crystallographic  $c$  and  $b$  axes emphasizing the different pore size distribution of the octagonal pores of the open-framework structure (the void spaces are represented by pale yellow spheres). Metal and ligand atoms are represented by balls and sticks, respectively (Cu, green; Mn, purple).

physi- or chemisorption processes, opening thus the way for future applications of porous magnets as magnetic sensors for host-guest molecular sensing.<sup>42</sup>

By following the same preparative route described above to synthesize the magnetic sponge of formula  $[\text{Na}(\text{H}_2\text{O})_4]_4\{\text{Mn}_4[\text{Cu}_2(\text{mpba})_2(\text{H}_2\text{O})_4]_3\} \cdot 56.5 \text{ H}_2\text{O}$ , we recently prepared an isoreticular analogue of formula  $[\text{Na}(\text{H}_2\text{O})_{3.25}]_4\{\text{Mn}_4[\text{Cu}_2(\text{Me}_3\text{mpba})_2(\text{H}_2\text{O})_{3.33}]_3\} \cdot 37 \text{ H}_2\text{O}$  [ $\text{Me}_3\text{mpba} = N,N'$ -2,4,6-trimethyl-1,3-phenylenebis(oxamate)] by the reaction of  $\text{Na}_4[\text{Cu}_2(\text{Me}_3\text{mpba})_2] \cdot 4\text{H}_2\text{O}$  and  $\text{Mn}(\text{NO}_3)_2 \cdot 4\text{H}_2\text{O}$  in water.<sup>28</sup> Unlike the related compound of formula  $\text{Na}_4\{\text{Mn}_4[\text{Cu}_2(\text{mpba})_2]_3\}$ , the anhydrous phase  $\text{Na}_4\{\text{Mn}_4[\text{Cu}_2(\text{Me}_3\text{mpba})_2]_3\}$  exhibits selective gas and vapour sorption behaviour together with a drastic variation of the long-range magnetic properties as a function of the adsorbed guest, constituting thus the first example of a genuine 3D porous magnet in the family of the oxamato-based CPs.<sup>14,15</sup>

The anionic 3D pillared, square/octagonal networks of  $[\text{Na}(\text{H}_2\text{O})_{3.25}]_4\{\text{Mn}_4[\text{Cu}_2(\text{Me}_3\text{mpba})_2(\text{H}_2\text{O})_{3.33}]_3\} \cdot 37 \text{ H}_2\text{O}$  and  $[\text{Na}(\text{H}_2\text{O})_4]_4\{\text{Mn}_4[\text{Cu}_2(\text{mpba})_2(\text{H}_2\text{O})_4]_3\} \cdot 56.5 \text{ H}_2\text{O}$  are topologically identical but they have different shapes because of the regular or flattened nature respectively, of the octagonal circuits in each case, as nicely illustrated by Fig. 10. Moreover, the resulting open-framework structure in this novel analogue presents a trimodal pore size distribution with small square pores but two types of large octagonal pores (Fig. 10a), instead of the bimodal one found in the parent compound (Fig. 10b). These medium and wide octagonal channels with approximate diameters of 1.5 and 2.2 nm respectively, result from the distinct orientation of the trimethyl-substituted phenylene spacers pointing inwards or outwards of the channels (steric size effect).

The percentage of potential void space per unit cell volume in  $[\text{Na}(\text{H}_2\text{O})_{3.25}]_4\{\text{Mn}_4[\text{Cu}_2(\text{Me}_3\text{mpba})_2(\text{H}_2\text{O})_{3.33}]_3\} \cdot 37 \text{ H}_2\text{O}$  is lower than in  $[\text{Na}(\text{H}_2\text{O})_4]_4\{\text{Mn}_4[\text{Cu}_2(\text{mpba})_2(\text{H}_2\text{O})_4]_3\} \cdot 56.5 \text{ H}_2\text{O}$  (60 vs. 70%), as expected because of the additional presence of methyl group substituents and further supported by the smaller amount of crystallisation water molecules. However, the trimethyl-substituted derivative presents two clear differences with respect to the non-substituted one that can have a large influence on their relative adsorptive properties: (i) larger diameters for the wide octagonal pores as a consequence of the different orientation of the phenylene spacers (which would be reflected in an increase of the accessible surface area of the MOF), and (ii) easier accessibility for the guest molecules to interact with the copper(II) ions within the wide octagonal channels since the phenylene spacers are pointing inwards the medium octagonal channels (Fig. 10a).

The accessible porosity of the anhydrous compound  $\text{Na}_4\{\text{Mn}_4[\text{Cu}_2(\text{Me}_3\text{mpba})_2]_3\}$  was also estimated by means of gas adsorption measurements, indicating a moderate  $\text{CO}_2/\text{CH}_4$  gas selectivity (Fig. 11a).<sup>28</sup> This situation clearly contrasts with that previously found for  $\text{Na}_4\{\text{Mn}_4[\text{Cu}_2(\text{mpba})_2]_3\}$ , where no gas or vapour sorption loadings were observed.<sup>27</sup> This dramatically different sorption behaviour was attributed to the larger accessible surface area present in

$\text{Na}_4\{\text{Mn}_4[\text{Cu}_2(\text{Me}_3\text{mpba})_2]_3\}$  and/or the possible collapse of the structure in  $\text{Na}_4\{\text{Mn}_4[\text{Cu}_2(\text{mpba})_2]_3\}$  under removal of the solvent water molecules. Other gas molecules like  $\text{H}_2$  or  $\text{N}_2$  were not adsorbed by  $\text{Na}_4\{\text{Mn}_4[\text{Cu}_2(\text{Me}_3\text{mpba})_2]_3\}$  at room temperature, suggesting that they do not interact with the host network and confirming thus the large selectivity of this system for the separation of small molecules.

Vapour adsorption/desorption isotherms showed a considerable adsorption of some solvents like water and methanol, whereas under similar conditions, no vapour adsorption was observed for other solvents such as ethanol or acetonitrile. This fact indicated a large selectivity for the sorption of small molecules by this compound and suggested that both the kinetic diameter and the interaction with the network play a key role in the sorption process. This large selectivity for small molecules and the growing interest in the development of energy efficient methods for the separation of azeotropic mixtures, led us to perform breakthrough experiments in a column packed with  $\text{Na}_4\{\text{Mn}_4[\text{Cu}_2(\text{Me}_3\text{mpba})_2]_3\}$ . The results obtained in the separation of a liquid azeotropic  $\text{CH}_3\text{CN}/\text{CH}_3\text{OH}$  solvent mixture (79:21 v/v) revealed that  $\text{CH}_3\text{CN}$  eluted very fast from the column (retention time close to zero), while  $\text{CH}_3\text{OH}$  was strongly retained (retention time of 12.70 min) (Fig. 11b).<sup>28</sup>

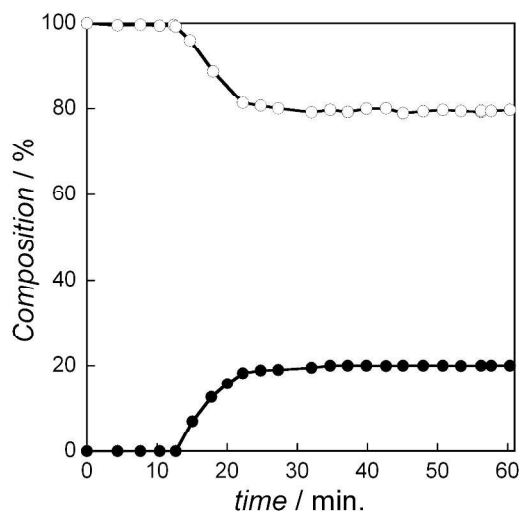
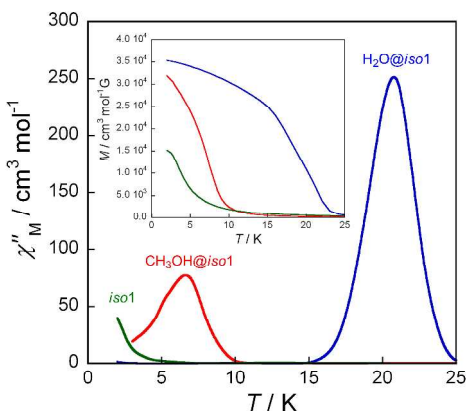


Fig. 11 Evolution of the  $\text{CH}_3\text{OH}$  (●) and  $\text{CH}_3\text{CN}$  (○) concentrations after feeding of a liquid azeotropic  $\text{CH}_3\text{CN}/\text{CH}_3\text{OH}$  mixture (79:21 v/v) through a column packed with the compound  $\text{Na}_4\{\text{Mn}_4[\text{Cu}_2(\text{Me}_3\text{mpba})_2]_3\}$ .

Finally, we also studied the influence of the sorption of small molecules in the overall magnetic behaviour. A paramagnetic to ferromagnetic phase transition was observed for the anhydrous phase  $\text{Na}_4\{\text{Mn}_4[\text{Cu}_2(\text{Me}_3\text{mpba})_2]_3\}$  at a rather low critical temperature ( $T_C$ ) of ca. 2.0 K, as revealed by both the alternating current (ac) magnetic susceptibility and direct current (dc) magnetisation measurements (Fig. 12). Interestingly, the value of the magnetic ordering temperature progressively shifts to higher values when solvents like methanol ( $T_C = 6.5 \text{ K}$ ) or water ( $T_C = 21 \text{ K}$ ) are adsorbed within the host framework. The observed variation in the magnetic

behaviour for the different adsorbates was repeated for several cycles of solvent adsorption/desorption with identical results, supporting thus the reversible nature of the adsorption/desorption processes and the fast interconversion between the different adsorbates. The differences observed in the magnetic properties of the different adsorbates are likely related to the axial binding and their removal of the solvent molecules ( $\text{H}_2\text{O}$  or  $\text{CH}_3\text{OH}$ ) from the first coordination sphere of the  $\text{Cu}^{\text{II}}$  ions.



**Fig. 12** Temperature dependence of the ac out-of-phase molar magnetic susceptibility ( $\chi_M''$ ) of *iso1* (green),  $\text{CH}_3\text{OH}@iso1$  (red), and  $\text{H}_2\text{O}@iso1$  (blue) with a  $\pm 4.0$  G field oscillating at 1000 Hz. The inset shows the temperature dependence of the magnetization ( $M$ ) of the three adsorbates.

The coexistence of a selective vapour and gas sorption behaviour and a solvent-dependent enhancing of the long-range magnetic ordering temperature allows for potential applications in magnetic sensing of small guest molecules for this new member of the family of porous magnets.<sup>42,43</sup>

## 5. Luminescent porous magnets

Among the wide variety of properties of interest that a given material can exhibit, luminescence attracts large attention due to its potential application in optical devices for lighting equipment and optical storage,<sup>44a-c</sup> optical switching,<sup>44d,e</sup> and sensing.<sup>44f,i</sup> At this respect, many groups are directing their efforts towards the preparation of luminescent materials with potential sensing applications. For instance, sensitive and selective detection of gas and vapour phase analytes can be particularly interesting because of their variety of applications in many different fields.

### 5.1 Luminescence and magnetic sensing in a 2D double-hexagonal CP

In a recent work,<sup>29</sup> we synthesized a novel manganese(II)-copper(II) 2D compound of formula  $\text{MV}[\text{Mn}_2\text{Cu}_3(\text{mpba})_3(\text{H}_2\text{O})_3] \cdot 20\text{H}_2\text{O}$ , where  $\text{MV}^{2+}$  is the methylviologen dicationic dye.<sup>45</sup> This compound exhibits highly selective gas sorption ability, luminescence capacity, and long-range magnetic ordering, constituting thus a unique example of luminescent porous magnet with potential

applications in host-guest chemical sensing of small molecules. In fact, a unique optical and magnetic switching behaviour is observed accompanying reversible solvation/desolvation and gas sorption/desorption processes.

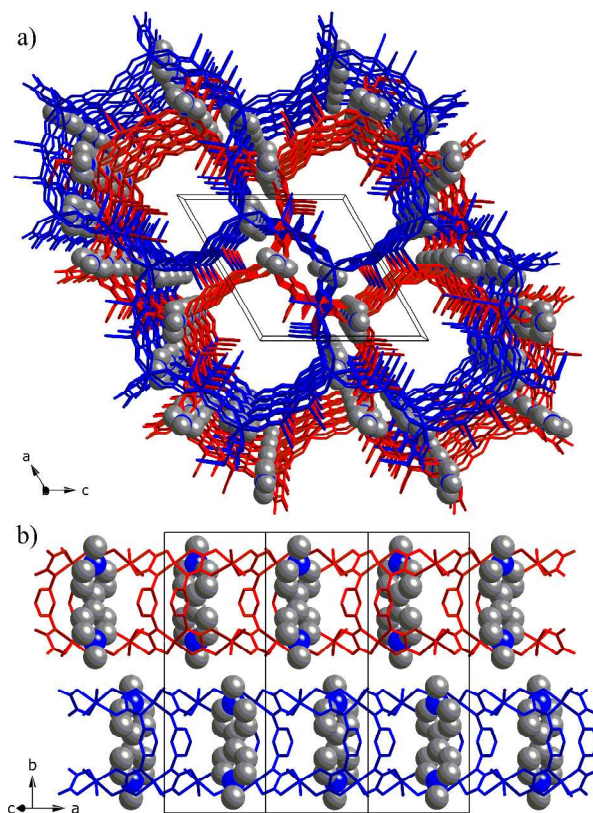


**Fig. 13** Perspective views of the crystal packing of adjacent double layers of  $\text{MV}[\text{Mn}_2\text{Cu}_3(\text{mpba})_3(\text{H}_2\text{O})_3] \cdot 20\text{H}_2\text{O}$  along the crystallographic  $b$  (a) and in the  $ab$  plane (b). The alternating  $A$  and  $B$  double layers are in red and blue colours, respectively. The  $\text{MV}^{2+}$  counteranions are represented as space filling spheres. The solvent water molecules have been omitted for clarity.

Its crystal structure consists of anionic 2D bimetallic networks made up by two adjacent oxamato-bridged  $\text{Mn}^{\text{II}}\text{Cu}^{\text{II}}_3$  flat irregular hexagonal layers of  $[6^3]$  hcb topology that are interconnected through two  $m$ -phenylene spacers between the  $\text{Cu}^{\text{II}}$  ions along the crystallographic  $b$  axis (Fig. 13). These adjacent double hexagonal layers closely stack above each other yielding small nanopores, which are occupied by hydrogen-bonded arrays of crystallization water molecules and the methylviologen cations (Fig. 13). The estimated empty volume without the crystallization water molecules is  $3179 \text{ \AA}^3$ , a value that represents up to *ca.* 43% of potential void per unit cell volume [ $V = 7414.7(18) \text{ \AA}^3$ ]. The  $\text{MV}^{2+}$  cations are situated very close to the anionic heterobimetallic double layers, establishing weak intermolecular (van der Waals and/or electrostatic) interactions between their pyridinium-nitrogen and the carboxylate-oxygen atoms which are coordinated to the  $\text{Cu}^{\text{II}}$  ions (Fig. 13b). This situation results in an effective approach between the anionic metal-organic network and the organic cations which are responsible for the cation templating effects that lead to the adoption of a lower symmetry ('non-

default') double layer 2D hexagonal architecture instead of the highest symmetry ('default') pillared 3D hexagonal one, where the two *m*-phenylene spacers between the Cu<sup>II</sup> ions would act as pillars in an alternately up and down disposition. Moreover, these weak interactions between the anionic metal-organic network and the organic cations would be ultimately responsible for the intriguing magnetic and luminescent sensing properties.

In fact, the study of the influence of the sorption of small molecules like solvent vapours and gases by this porous material revealed a unique magnetic and luminescent switching behaviour, which can be summarised as follows:

(i) The active anhydrous phase MV[Mn<sub>2</sub>Cu<sub>3</sub>(mpba)<sub>3</sub>] shows a long-range ferromagnetic ordering at a rather low critical temperature ( $T_C$ ) of 2.0 K, as found earlier for related oxamato-based heterobimetallic manganese(II)-copper(II) magnets with a single layer hexagonal structure (see section 2.2).<sup>15</sup> Upon solvent vapour adsorption, the magnetic ordering temperature progressively shifts towards higher values depending on the adsorbed guest molecule: MeOH ( $T_C \approx 5.0$  K) and H<sub>2</sub>O ( $T_C \approx 19.0$  K). The observed variation in the magnetic behaviour along this series of adsorbates can be repeated for several cycles of solvent adsorption/desorption with identical results. This supports the reversible nature of the adsorption/desorption processes and the fast interconversion between the dehydrated phase and the two different adsorbates. The differences observed in their magnetic properties would be related to the presence of weak dipolar ("through-space") and/or hydrogen-bonded ("through-bond") magnetic interactions between adjacent double layers through the solvent molecules, as revealed by the crystal structure of the hydrated phase MV[Mn<sub>2</sub>Cu<sub>3</sub>(mpba)<sub>3</sub>(H<sub>2</sub>O)<sub>3</sub>] · 20H<sub>2</sub>O, which are ultimately responsible for the long-range 3D ferromagnetic order of the weakly-interacting ferrimagnetic heterobimetallic double layers.<sup>27-29</sup>

(ii) The active anhydrous phase MV[Mn<sub>2</sub>Cu<sub>3</sub>(mpba)<sub>3</sub>] shows a bright UV and visible light emission at 330 and 586 nm (upon excitation at 225 and 400 nm, respectively), which makes it the first example of an oxamato-based luminescent magnet reported in the literature. The presence of highly ordered MV<sup>2+</sup> cations filling the nanopores of this material afforded the observed luminescent properties. In fact, although MV<sup>2+</sup> in solution does not fluoresce, a bright UV light emission at around 330 nm had been already reported when encapsulated in porous solids.<sup>45</sup> Herein, the dual UV and visible light emission is attributed to the MV<sup>2+</sup> species interacting with the Cu<sup>II</sup> ions.<sup>45a</sup> The most interesting feature, however, lies in the fact that a clear blue-shift of the lower energy visible emission from 586 to 544 nm occurs upon rehydration at 33% water loading (Fig. 14a). In addition, a good linear relationship is found between the shift in the emission wavelength and the degree of framework hydration. Similarly, a smaller but non-negligible blue-shift of the lower energy visible emission from 586 to 580 nm was observed when loading the anhydrous compound with methanol (data not shown). The observed solvent-induced variation of the luminescence properties

strongly supports the occurrence of small changes in the Cu<sup>II</sup>-MV<sup>2+</sup> distance during the adsorption-desorption processes.

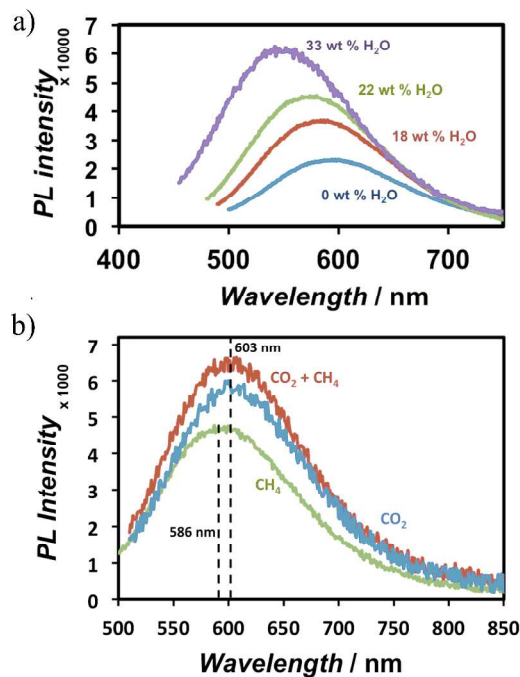


Fig. 14 (a) Emission spectra of **1** ( $\lambda_{exc} = 400$  nm) during adsorption at different water loadings. (b) Emission spectra of the anhydrous derivative of MV[Mn<sub>2</sub>Cu<sub>3</sub>(mpba)<sub>3</sub>] in CH<sub>4</sub>, CO<sub>2</sub> and an equimolar CO<sub>2</sub>:CH<sub>4</sub> mixture at 1 bar.

(iii) The active anhydrous phase MV[Mn<sub>2</sub>Cu<sub>3</sub>(mpba)<sub>3</sub>] shows a relatively large and selective gas adsorption for CO<sub>2</sub> against CH<sub>4</sub>, constituting thus a unique example of luminescent porous magnet. Challenged by these surprising results, additional emission studies were performed under different pure and mixture gas atmospheres. The corresponding emission spectra of the anhydrous phase MV[Mn<sub>2</sub>Cu<sub>3</sub>(mpba)<sub>3</sub>] under 1 bar of pure CH<sub>4</sub>, 1 bar of pure CO<sub>2</sub>, and 1.5 bar of a 1:1 CO<sub>2</sub>/CH<sub>4</sub> mixture can be seen in Fig. 14b. The emission spectrum after CH<sub>4</sub> treatment still corresponds with that of the dehydrated framework, further demonstrating that CH<sub>4</sub> does not adsorb. In contrast, a considerable red-shift is observed when CO<sub>2</sub> is adsorbed. For a CO<sub>2</sub>/CH<sub>4</sub> mixture, the results are similar to those obtained with pure CO<sub>2</sub>. Since CH<sub>4</sub> does not adsorb on the dehydrated framework, the luminescence response to CO<sub>2</sub> is similar as for the single gas experiment, demonstrating that CO<sub>2</sub> can be detected in the presence of non-adsorbing gases (like methane or others). These results highlight the high selectivity of this material as a CO<sub>2</sub> sensor, even in the presence of other analytes. Another relevant feature of **1** is that the adsorption of CO<sub>2</sub> results in a clear red-shift emission, whereas the presence of H<sub>2</sub>O and CH<sub>3</sub>OH in the framework produces a blue-shift emission. This is likely due to the differences in the specific adsorption sites for CO<sub>2</sub>, CH<sub>3</sub>OH and H<sub>2</sub>O and to the different adsorption capacity for these adsorbates. This difference in the response is very important, since it probes that this system is

not only adsorption loading sensitive but also specific, allowing the identification of adsorbates and fulfilling thus, some of the key principles which were outlined by Kitagawa for its use in chemical sensing.<sup>43b</sup>

In summary, by combining the well-known emitting properties of the  $MV^{2+}$  cation guest with the magnetic properties of the oxamato-bridged bimetallic open-framework host with shape selective sorption behaviour, identification of small molecules is possible by direct observation of the host-guest interactions. The combination of these thrilling porous, optical, and magnetic properties makes it an ideal molecule-based multifunctional material for specific chemical sensing applications.<sup>42,43</sup>

## 6. Conclusions and outlook

The advantages that the well-known but barely used *N*-substituted aromatic oligo(oxamato) ligands can offer for the construction of MMCPs have been outlined in this feature article. Oxamato-based oligonuclear metal complexes, from mono- to di- and trinuclear species (see Scheme 1), can be used as metal-organic ligands (metalloligands) for the preparation of multidimensional *nD* ( $n = 1-3$ ) coordination polymers (CPs) or metal-organic frameworks (MOFs) with interesting magnetic properties.

Additional physical properties can be introduced in these materials by means of either the ligand design or the appropriate choice of the required counteraction, affording the first examples of oxamato-based multifunctional magnetic coordination polymers (MMCPs) which include: (i) optically-active chiral magnets (including the first example of enantiopure 1D chiral single-chain magnets); (ii) dynamic porous magnets; and (iii) luminescent porous magnets. Overall, these results show that the oxamate ligands constitute a rational and suitable alternative route to prepare molecule-based multifunctional magnetic materials, an avenue that inexplicably was rarely explored in the widespread field of porous coordination polymers (PCPs) or metal-organic frameworks (MOFs).<sup>4-8</sup>

Indeed, we feel that only a small fraction of the potentialities of oxamato-based MMCPs (those presented in this contribution) have been explored, most of the iceberg being still hidden beneath the surface. In an attempt to highlight the vast perspectives for the near future, let us briefly advance some of the very recent results issued from our two current research avenues in this area.

### 6.1 Electro- and photoactive CPs as magnetic sensors

PCPs are well-recognised for their use in gas storage and separation but, however, their applications for drug delivery, detoxification of radioactive and heavy metals and pesticides are much less explored. Moreover, there are relatively fewer reports on their capacity for tentatively acting as *magnetic sensors* through adsorption/desorption of specific guest molecules with reversible and dynamic changes of their open-framework structures and magnetic properties. In fact, the

preparation of this type of dynamic porous magnets with a wide range of miscellaneous sensing applications presents some major challenges.

Our strategy for the design of a new family of dynamic porous magnets with potential applications as magnetic sensors is based on the use of oxamate-containing dicopper(II) complexes with  $\pi$ -conjugated aromatic spacers such as oligophenylene (OPs), oligophenyleneethyne (OPEs), oligoacenes (OAs), oligoacenoquinones (OAQs), oligophenylenevinylenes (OPVs), and oligoazobenzenes (OABs) (see Scheme 1), which can act as metalloligands toward first-row transition metal ions such as manganese(II), cobalt(II) and nickel(II) leading to the corresponding PCPs.

The strategy for the rational design of this new family of dynamic porous magnets for magnetic sensing is based on two advantages that the oxamate-based dicopper(II) metallacyclophane precursors may show, as mentioned in Section 2.1. On the one hand, we have demonstrated the unique ability of OPs and OPEs to act as “molecular magnetic wires” (MMWs), being efficient in the transmission of magnetic exchange interactions between the two metal centres separated by very long intermetallic distances in the corresponding oxamato-based dicopper(II) oligophenyleneophanes and oligophenyleneethynophanes.<sup>19b,e</sup> On the other hand, the oxamato-based dicopper(II) oligoacenoquinophanes and oligoacenoquinophanes act as “molecular magnetic switches” (MMSs), because of the non-innocent character of the aromatic spacers as regarding their photo- or electroactive character.<sup>19d,g</sup> Thus, they would present two metastable states (‘ON/OFF’) with totally different magnetic properties which can be reached in a reversible manner through photochemical or redox processes. The spins of the magnetic centres are ferromagnetically coupled in one of the states (‘ON’), whereas they are antiferromagnetically coupled or magnetically isolated in the other state (‘OFF’).

Indeed, the design and synthesis of exchange-coupled, oxamato-based dicopper(II) complexes exhibiting a magnetic bistable behaviour is a corner stone in the building of dynamic porous magnets for chemical sensing because the changes in the magnetic properties of the host framework can be used to monitor the binding and/or transformation of the organic guest. Several points should be considered in order to obtain a new family of magnetic sensors of the host-guest type depending on the nature of the target chemical sensing application.

Firstly, we plan the synthesis of neutral oxamato-bridged heterobimetallic 2D CPs with rod-like OP and OPE spacers as dynamic porous magnets for gas storage and separation, as those reported earlier for the permethylated derivative of the shorter dicopper(II) paracyclophane possessing a brick-wall architecture (Fig. 15a).<sup>14b,c</sup> So, the systematic variation of the length of the aromatic spacers of the oxamate-containing dicopper(II) precursors can modulate the size of the channels which in the last term, would afford a selective gas separation (Fig. 11b). Moreover, the longer OP and OPE spacers, like 1,4-di(4-phenyl)phenylene and 1,4-di(4-phenylethynyl)phenylene, are suitable candidates to afford quite big channels with large

storage capacity for gases with potential oxidising ( $O_2$ ) or reducing ( $H_2$ ) power.

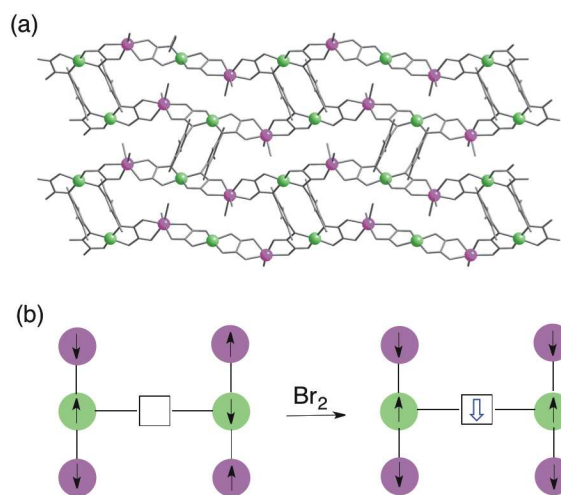


**Fig. 15** (a) Crystal structure of  $[Mn_2Cu_2(Me_4ppba)_2(H_2O)_4]_n \cdot nH_2O$  showing the neutral 2D rectangular layer of brick-wall architecture. Metal and ligand atoms are represented by balls and sticks, respectively (Cu, green; Mn, purple). (b) Proposed magnetic electroswitching in neutral oxamato-bridged 2D CPs built from redox-active, antiferromagnetically coupled dicopper(II) precursors acting as magnetic sensors of the 'host-guest' type for gas storage and separation.

So, for instance, our preliminary studies on the sorption properties of the oxamato-based manganese(II)-copper(II) 2D CPs with permethylated dicopper(II) paracyclophane cores show a unique magnetic switching behaviour after bromine gas adsorption. So, a change from non-magnetic to magnetic layer ground state occurs upon  $Br_2$  oxidation of the tetramethyl-substituted *p*-phenylene spacers (Fig. 15b), as reported earlier for the dicopper(II) precursor itself,<sup>19f</sup> constituting thus a unique example of electroactive porous magnet which can be used as magnetic sensor.

Secondly, we also plan the synthesis of neutral oxamato-bridged heterometallic 2D coordination polymers with photo-active OPVs and OABs spacers as dynamic porous magnets for drug delivery, as depicted by Fig. 16. In this sense, the shorter OPV and OAB spacers such as stilbene and azobenzene are interesting candidates for small drugs storage and delivery by taking advantage of their well-known *cis-trans* photoisomerization to modulate the pore size upon irradiation ('photo-gated pores'). These include either non-steroidal anti-inflammatory organic drugs (ibuprofen, naproxen, aspirin, etc.) or metalloorganic molecules with pharmacological potential (*cis*-platin). In both cases, the spin of the metal centers are antiferromagnetically coupled in the planar *trans* isomer ('ON' state), whereas they are magnetically isolated in the non-planar *cis* one ('OFF' state). Indeed, these changes in the magnetic properties of the host framework can be used to monitor the binding of the organic guest (magnetic sensing).

Thirdly, we plan to investigate the ability of anionic oxamato-bridged heterobimetallic 3D CPs, as those earlier reported for the permethylated derivative of the shorter dicopper(II) metacyclophane possessing a pillared

square/octagonal architecture (Fig. 10a and c) to act as selective ion exchangers for detoxification of radioactive (Cs, U and Th) and heavy metal (Pb and Hg) atoms, as depicted by Fig. 17. In fact, we have recently shown that the weakly coordinated  $Na^+$  cations in the oxamate-bridged porous magnet of formula  $[Na(H_2O)_4]_4\{Mn_4[Cu_2(Me_3mpba)_2(H_2O)_4]_3\} \cdot 56.5 H_2O$  (Fig. 12a) can be easily replaced by other alkaline ( $Li^+$  or  $K^+$ ) and alkaline-earth cations ( $Mg^{2+}$  or  $Ca^{2+}$ ) as well as transition metal ions ( $Ni^{2+}$  or  $Co^{2+}$ ) or lanthanide cations, with a concomitant change in the long-range magnetic ordering temperature.

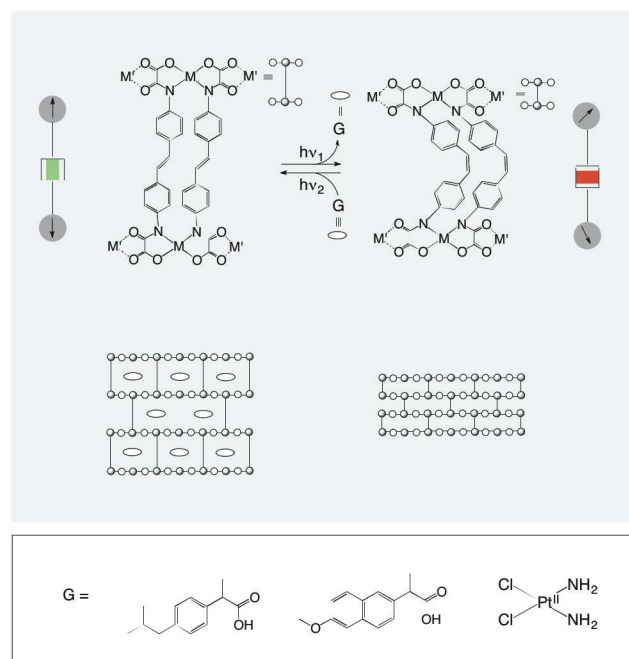


**Fig. 16** Proposed photomagnetic switching in neutral oxamato-bridged 2D CPs built from photo-active, antiferromagnetically coupled dicopper(II) precursors acting as magnetic sensors of the 'host-guest' type for drug delivery.

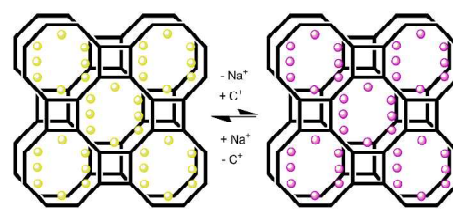
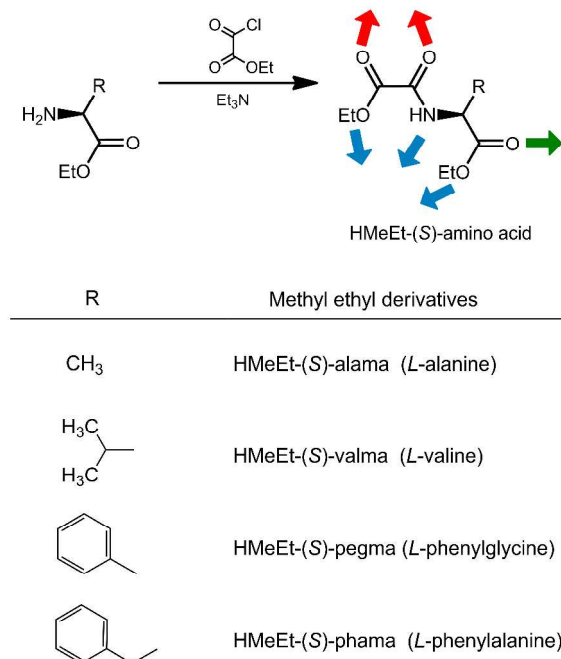


**Fig. 17** Cation exchange approach for the replacement of sodium cations in the anionic oxamato-bridged 3D CPs built from ferromagnetically coupled dicopper(II) precursors with pollutant agents such as radioactive isotopes and heavy metals.

## 6.2 Multifunctional chiral *bio*-coordination polymers

This last point, describing our current work with a novel family of bio-inspired carboxylate-functionalised oxamato ligands, deserves especial attention. Among the wide variety of physical properties that a MMCP can exhibit, those involving spatial asymmetry are especially appealing because of the intriguing properties associated to chirality. In this sense, MMCPs

exhibiting chiroptical and/or magnetic properties are a potentially new generation of chiral separation materials but have also relevant in the development of new classes of chiroptical probes and magnetic sensors. Although we have already successfully prepared the first example of oxamato-based optically-active chiral 3D magnetic polymers (see section 3.1.2), an accurate control of the final structure of the CP, and thus, of the chiral and magnetic properties, is still a challenge. This is particularly true from a synthetic point of view, since we cannot completely ensure the chiral induction from the cation to the stereochemistries of the metal ions by following the cation-assisted chiral-induction.<sup>32</sup>



**Scheme 2.** Synthetic route for the preparation of the methyl ethyl derivatives of the chiral (*S*)-*N*-oxalamino acids as a function of the starting natural or not amino acid precursors. The red, blue and green arrows represent the three different coordination modes of these versatile ligands.

In order to overcome these severe limitations, we are following the same synthetic strategy used in section 3.1.1 which is based on the use of a new family of enantiopure, oxamato-based ligands derived from natural and non-natural amino acids (Scheme 2). The resultant anionic coordination networks could tentatively exhibit chirality and host a wide variety of functional cations in their channels giving rise to new classes of hybrid materials and multifunctional molecule-based magnets presenting new physical properties such as second-order optical nonlinearities, magnetochiral-dichroism or ferroelectricity.<sup>33-35</sup>

The methyl ethyl derivatives of the (*S*)- and (*R*)-*N*-oxalamino acids can be easily obtained in an enantiopure form from the reaction of the methyl ester derivatives of the corresponding amino acids with ethyl oxalyl chloride as shown in Scheme 2. The most remarkable point of this new generation of ligands together with their intrinsic chiral nature, lies in their great versatility as well as large variety of coordination modes

they can adopt. For example, as a part of our preliminary work, we reported how the Cu<sup>2+</sup>-mediated self-assembly of the putative tridentate HMeEt-(*S*)- and HMeEt-(*R*)-valma proligands in basic aqueous solutions leads to the formation of two homochiral anionic hexacopper(II) wheels of general formula (Me<sub>4</sub>N)<sub>6</sub>[Cu<sup>II</sup><sub>6</sub>L<sub>6</sub>]·7H<sub>2</sub>O [Me<sub>4</sub>N<sup>+</sup> = tetramethyl ammonium cation; L = (*S*)-valma and (*R*)-valma] that crystallize in the same chiral space group *P*6(3) of the hexagonal system (Fig. 18).<sup>46</sup>

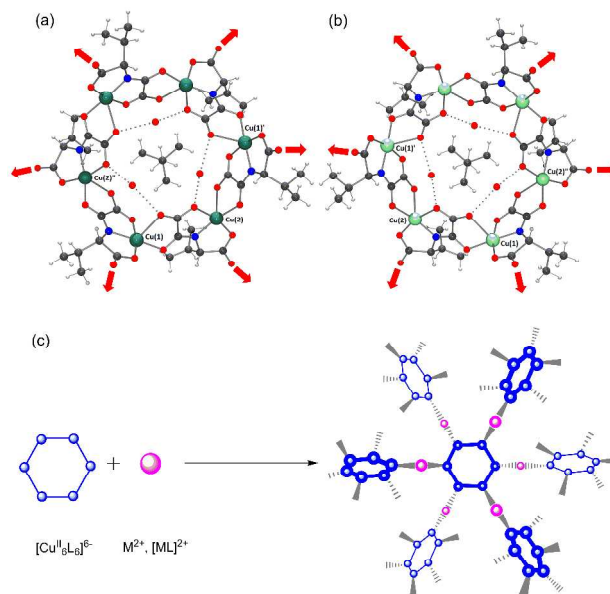


**Fig. 18** Top views of the anionic hexacopper(II) rings of (Me<sub>4</sub>N)<sub>6</sub>[Cu<sup>II</sup><sub>6</sub>L<sub>6</sub>]·7H<sub>2</sub>O [L = (*S*)-valma (a) and (*R*)-valma (b)]. The metal atoms of A or C chirality are shown in deep and pale green colours, respectively. (c) Proposed structure of the 3D CP resulting from the self-assembly of the hexacopper(II) chiral rings and M<sup>2+</sup> ions or square metal-organic cationic complexes.

These polymeric wheels present up to six free carbonyl groups from the valine residues at the outer rim (red arrows in Fig. 18) that can coordinate to other metal ions or coordinatively unsaturated metal complexes to afford high-dimensional PCPs. (Fig. 18). In addition, the chiral nature of the ligand itself which is transferred to the coordination spheres of the metal ions, allow us to predict that chiral CPs, with large chiral channels, could be obtained. This original two-step programmed method affords a better control of both the final architecture and the enantiopure nature of the resulting bio-CP.<sup>47</sup> Finally, these new chiral materials would provide fascinating possibilities in enantiomeric separation and could exhibit NLO and/or ferroelectric properties when a polar guest molecule is introduced.<sup>33-35</sup>

### Acknowledgements

This work was supported by the MICINN (Spain) (Project CTQ2010-15364) and the Generalitat Valenciana (Spain) (Projects PROMETEO/2009/108, GV/2012/051 and ISIC/2012/002). T. G. thanks the Universitat de València for a predoctoral contract. Thanks are also extended to the MICINN Ramón y Cajal Program (E. P.) and 'Factoría de Cristalización'

Consolider-Ingenio Project CSD2006-00015 (J. P.) for postdoctoral contracts. We acknowledge all the coworkers who have collaborated in this area and whose names appear in the reference list below. Particular thanks go to our colleagues from the groups of Drs Yves Journaux (Université Pierre et Marie Curie) and Jorge Gascon (Delft University of Technology), whose contributions and enthusiasm have been essential to the birth and further development of our research on oxamato-based multifunctional magnetic coordination polymers. We are especially thankful to Drs Rafael Ruiz-García and Joan Cano (Universitat de València) for unselfish help and continuous interest in this work.

### Notes and references

<sup>a</sup> Departament de Química Inorgànica/Instituto de Ciencia Molecular (ICMol). Universitat de València. 46980 Paterna, València, Spain. Fax: 343543273; Tel: 343544442; E-mail: [Emilio.Pardo@uv.es](mailto:Emilio.Pardo@uv.es) (E.P.).

<sup>b</sup> Laboratorio de Rayos X y Materiales Moleculares, Departamento de Física Fundamental II, Universidad de La Laguna, E-38201 Tenerife, Spain.

1 O. Kahn, *Molecular Magnetism*, VCH, New York, USA, 1993.

2 (a) *Magnetism: A Supramolecular Function*, ed. O. Kahn, NATO ASI Series C, Kluwer, Dordrecht, Germany, 1995, vol. 484; (b) *Molecular Magnetism: From Molecular Assemblies to the Devices*, eds. E. Coronado, P. Delhaès, D. Gatteschi and J. S. Miller, NATO ASI Series E, Kluwer, Dordrecht, Germany, 1995, vol. 321; (c) *Supramolecular Engineering of Synthetic Metallic Materials*, J. Veciana, C. Rovira and D. Amabilino, NATO ASI Series C, Kluwer, Dordrecht, Germany, 1998, vol. 518; (d) *Magnetism: Molecules to Materials*, eds. J. S. Miller and M. Drillon, Wiley-VCH, Weinheim, Germany, 2001, Vols. I-V; (e) *Multifunctional Molecular Materials*, ed. L. Ouahab, Pan Stanford Publishing, Singapore, 2013; (e) *Electrons in Molecules. From Basic Principles to Molecular Electronics*, eds. J. P. Launay and M. Verdager, Oxford University Press, Oxford, United Kingdom, 2014.

3 (a) M. M. Turnbull, T. Sugimoto and L. K. Thompson, *Molecule-Based Magnetic Materials*. American Chemical Society, Washington, DC, 1996; (b) E. Coronado, F. Palacio and J. Veciana, *Angew. Chem. Int. Ed.*, 2003, **42**, 2570 and references therein.

4 C. Janiak and J. K. Vieth, *New J. Chem.*, 2010, **34**, 2366, and references therein.

5 B. F. Abrahams, B. F. Hoskins, D. M. Michail and R. Robson, *Nature*, 1994, **369**, 727.

6 S. Decurtins, H. W. Schmalte, P. Schneuwly and H. R. Oswald, *Inorg. Chem.*, 1993, **32**, 1888.

7 (a) G. De Munno, M. Julve, F. Nicolo, F. Lloret, J. Faus, R. Ruiz and E. Sin, *Angew. Chem. Int. Ed. Engl.*, 1993, **32**, 613; (b) G. De Munno, M. Julve, G. Viau, F. Lloret, J. Faus and D. Viterbo, *Angew. Chem. Int. Ed. Engl.*, 1996, **35**, 1748; (c) F. Lloret, G. De Munno, M. Julve, J. Cano, R. Ruiz and A. Caneschi, *Angew. Chem. Int. Ed. Engl.*, 1998, **37**, 135.

8 O. M. Yaghi, M. O'Keeffe, N. W. Ockwig, H. K. Chae, M. Eddaoudi and J. Kim, *Nature*, 2003, **423**, 705.

9 (a) D. Maspoch, D. Ruiz-Molina and J. Veciana, *Chem. Soc. Rev.*, 2007, **36**, 770; (b) M. Kurmoo, *Chem. Soc. Rev.*, 2009, **38**, 1353; (c) P. Dechambenoit and J. R. Long, *Chem. Soc. Rev.*, 2011, **40**, 3249.

10 (a) L. G. Beauvais and J. R. Long, *J. Am. Chem. Soc.*, 2002, **124**, 12096; (b) S. S. Kaye and J. R. Long, *J. Am. Chem. Soc.*, 2005, **127**, 6506; (c) S. S. Kaye, H. J. Choi and J. R. Long, *J. Am. Chem. Soc.*, 2008, **130**, 16921; (d) L. J. Murray, M. Dinca and J. R. Long, *Chem. Soc. Rev.*, 2009, **38**, 1294; (e) H. Tokoro and S.-I. Ohkoshi, *Dalton Trans.*, 2011, **40**, 6825; (f) S.-I. Ohkoshi and H. Tokoro, *Acc. Chem. Res.*, 2012, **45**, 1749.

11 (a) E. Pardo, C. Train, G. Gontard, K. Boubekeur, O. Fabelo, H. Liu, B. Dkhil, F. Lloret, K. Nakagawa, H. Tokoro, S.-I. Ohkoshi and M. Verdager, *J. Am. Chem. Soc.*, 2011, **133**, 15328; (b) E. Pardo, C. Train, H. Liu, L. M. Chamoreau, B. Dkhil, K. Boubekeur, F. Lloret, K. Nakatani, H. Tokoro, S.-I. Ohkoshi and M. Verdager, *Angew. Chem. Int. Ed.*, 2012, **51**, 8356; (c) C. Train, R. Gheorghe, V. Krstic, L. M. Chamoreau, N. S. Ovanesyan, G. L. J. A. Rikken, M. Gruselle and M. Verdager, *Nat. Mater.*, 2008, **9**, 729; (d) E. Coronado, J. R. Galán-Mascarós, C. J. Gómez-García and V. Laukhin, *Nature*, 2000, **408**, 447.

12 (a) S. R. Batten and R. Robson, *Angew. Chem. Int. Ed.*, 1998, **37**, 1460; (b) G. Férey, *Chem. Soc. Rev.*, 2008, **37**, 191; (c) N. L. Rosi, M. Eddaoudi, J. Kim, M. O'Keeffe and O. M. Yaghi, *CrystEngComm*, 2002, **4**, 401; (d) J. R. Long and O. M. Yaghi, *Chem. Soc. Rev.*, 2009, **38**, 1213, and references therein; (e) S. Kitagawa and R. Matsuda, *Coord. Chem. Rev.*, 2007, **251**, 2490; (f) D. Bradshaw, J. B. Claridge, E. J. Cussen, T. J. Prior and M. J. Rosseinsky, *Acc. Chem. Res.*, 2005, **38**, 273.

13 (a) E. Pardo, R. Ruiz-García, J. Cano, X. Ottenwaelde, R. Lescouëzec, Y. Journaux, F. Lloret and M. Julve, *Dalton Trans.*, 2008, 2780; (b) M.-C. Dul, E. Pardo, R. Lescouëzec, Y. Journaux, J. Ferrando-Soria, R. Ruiz-García, J. Cano, M. Julve, F. Lloret, D. Cangussu, C. L. M. Pereira, H. O. Stumpf, J. Pasán and C. Ruiz-Pérez, *Coord. Chem. Rev.*, 2010, **254**, 2281.

14 (a) M. Verdager, O. Kahn, M. Julve and A. Gleizes, *Nouv. J. Chim.*, 1985, **9**, 325; (b) C. L. M. Pereira, E. F. Pedroso, H. O. Stumpf, M. A. Novak, L. Ricard, R. Ruiz-García, E. Rivière and Y. Journaux, *Angew. Chem. Int. Ed.*, 2004, **43**, 956; (c) J. Ferrando-Soria, J. Pasán, C. Ruiz-Pérez, Y. Journaux, M. Julve, F. Lloret, J. Cano and E. Pardo, *Inorg. Chem.*, 2011, **50**, 8694; (d) J. Ferrando-Soria, T. Grancha, J. Pasán, C. Ruiz-Pérez, L. Cañadillas-Delgado, Y. Journaux, M. Julve, J. Cano, F. Lloret and E. Pardo, *Inorg. Chem.*, 2012, **51**, 7019; (e) E. Pardo, D. Cangussu, M.-C. Dul, R. Lescouëzec, P. Herson, Y. Journaux, E. F. Pedroso, C. L. M. Pereira, M. C. Muñoz, R. Ruiz-García, J. Cano, P. Amorós, M. Julve, and F. Lloret, *Angew. Chem. Int. Ed.* 2008, **47**, 4211; (f) D. Cangussu, E. Pardo, M.-C. Dul, R. Lescouëzec, P. Herson, Y. Journaux, E. F. Pedroso, C. L. M. Pereira, H. O. Stumpf, M. C. Muñoz, R. Ruiz-García, J. Cano, M. Julve and F. Lloret, *Inorg. Chim. Acta*, 2008, **361**, 3394; (g) H. O. Stumpf, L. Ouahab, Y. Pei, D. Grandjean and O. Kahn, *Science*, 1993, **261**, 447.

15 J. Ferrando-Soria, T. Grancha, M. Julve, J. Cano, F. Lloret, Y. Journaux, J. Pasán, C. Ruiz-Pérez and E. Pardo, *Chem. Commun.*, 2012, **48**, 3539.

16 E. Pardo, I. Morales-Osorio, M. Julve, F. Lloret, J. Cano, R. Ruiz-García, J. Pasán, C. Ruiz-Pérez, X. Ottenwaelde and Y. Journaux, *Inorg. Chem.*, 2004, **43**, 7594.

17 (a) E. Pardo, R. Ruiz-García, F. Lloret, J. Faus, M. Julve, Y. Journaux, F. S. Delgado and C. Ruiz-Pérez, *Adv. Mater.*, 2004, **16**,

- 1597; (b) E. Pardo, R. Ruiz -García, F. Lloret, J. Faus, M. Julve, Y. Journaux, M. A. Novak, F. S. Delgado and C. Ruiz-Pérez, *Chem. Eur. J.*, 2007, **13**, 2054; (c) J. Ferrando-Soria, E. Pardo, R. Ruiz-García, J. Cano, F. Lloret, M. Julve, Y. Journaux, J. Pasán and C. Ruiz-Pérez, *Chem. Eur. J.*, 2011, **17**, 2176.
- 18 M.-C. Dul, R. Lescouëzec, L. M. Chamoreau, Y. Journaux, R. Carrasco, M. Castellano, R. Ruiz-García, J. Cano, F. Lloret, M. Julve, C. Ruiz-Pérez, O. Fabelo and E. Pardo, *CrystEngComm*, 2012, **14**, 5639.
- 19 (a) I. Fernández, R. Ruiz, J. Faus, M. Julve, F. Lloret, J. Cano, X. Ottenwaelder, Y. Journaux and M. C. Muñoz, *Angew. Chem., Int. Ed.*, 2001, **40**, 3039; (b) E. Pardo, J. Faus, M. Julve, F. Lloret, M. C. Muñoz, J. Cano, X. Ottenwaelder, Y. Journaux, R. Carrasco, G. Blay, I. Fernández and R. Ruiz-García, *J. Am. Chem. Soc.*, 2003, **125**, 10770; (c) E. Pardo, R. Carrasco, R. Ruiz-García, M. Julve, F. Lloret, M. C. Muñoz, Y. Journaux, E. Ruiz and J. Cano, *J. Am. Chem. Soc.*, 2008, **130**, 576; (d) M. Castellano, J. Ferrando-Soria, E. Pardo, M. Julve, F. Lloret, C. Mathonière, J. Pasán, C. Ruiz-Pérez, L. Cañadillas-Delgado, R. Ruiz-García and J. Cano, *Chem. Commun.*, 2011, **47**, 11035. (e) J. Ferrando-Soria, M. Castellano, R. Ruiz-García, J. Cano, M. Julve, F. Lloret, J. Pasán, C. Ruiz-Pérez, L. Cañadillas-Delgado, Y. Li, Y. Journaux and E. Pardo, *Chem. Commun.*, 2012, **48**, 8401; (f) M. Castellano, R. Ruiz-García, J. Cano, M. Julve, F. Lloret, Y. Journaux, G. De Munno and D. Armentano, *Chem. Commun.*, 2013, **49**, 3534; (g) W. D. do Prim, W. X. C. Oliveira, M. A. Ribeiro, E. N. de Faria, I. F. Teixeira, H. O. Stumpf, R. M. Lago, C. L. M. Pereira, C. B. Pinheiro, J. C. D. Figueiredo-Júnior, W. C. Nunes, P. P. de Souza, E. F. Pedroso, M. Castellano, J. Cano and M. Julve, *Chem. Commun.*, 2013, **49**, 10778; (h) F. R. Fortea-Pérez, I. Schlegel, M. Julve, D. Armentano, G. De Munno and S. E. Stiriba, *J. Organomet. Chem.*, 2013, **743**, 102.
- 20 (a) Y. Pei, M. Verdaguer, O. Kahn, J. Sletten and J. P. Renard, *J. Am. Chem. Soc.*, 1986, **108**, 7428; (b) Y. Pei, M. Verdaguer, O. Kahn, J. Sletten and J. P. Renard, *Inorg. Chem.*, 1987, **26**, 138; (c) O. Kahn, Y. Pei, M. Verdaguer, J. P. Renard and J. Sletten, *J. Am. Chem. Soc.*, 1988, **110**, 782.
- 21 (a) B. Cervera, J. L. Sanz, M. J. Ibáñez, G. Vila, F. Lloret, M. Julve, R. Ruiz, X. Ottenwaelder, A. Aukauloo, S. Poussereau, Y. Journaux and M. C. Muñoz, *J. Chem. Soc., Dalton Trans.*, 1998, 781; (b) A. Aukauloo, X. Ottenwaelder, R. Ruiz, Y. Journaux, Y. Pei, E. Rivière, B. Cervera and M. C. Muñoz, *Eur. J. Inorg. Chem.*, 1999, 209; (c) A. Aukauloo, X. Ottenwaelder, R. Ruiz, S. Poussereau, Y. Pei, Y. Journaux, P. Fleurat, F. Volatron, B. Cervera and M. C. Muñoz, *Eur. J. Inorg. Chem.*, 1999, 1067; (d) K. E. Berg, Y. Pellegrin, G. Blondin, X. Ottenwaelder, Y. Journaux, M. M. Canovas, T. Mallah, S. Parsons and A. Aukauloo, *Eur. J. Inorg. Chem.*, 2002, 323; (e) X. Ottenwaelder, R. Ruiz-García, G. Blondin, R. Carrasco, J. Cano, D. Lexa, Y. Journaux and A. Aukauloo, *Chem. Commun.*, 2004, 504.
- 22 (a) Y. Pei, Y. Journaux, A. Dei, O. Kahn and D. Gatteschi, *J. Chem. Soc., Chem. Commun.*, 1986, 1300; (b) Y. Pei, Y. Journaux and O. Kahn, *Inorg. Chem.*, 1988, **27**, 399;
- 23 (a) A. Caneschi, D. Gatteschi, N. Lalioti, C. Sangregorio, R. Sessoli, G. Venturi, A. Vindigni, A. Rettori, M. G. Pini and M. Novak, *Angew. Chem. Int. Ed. Engl.*, 2001, **40**, 1760; (b) R. Clérac, H. Miyasaka, M. Yamashita and C. Coulon, *J. Am. Chem. Soc.*, 2002, **124**, 12837; (c) R. Lescouëzec, J. Vaissermann, C. Ruiz-Pérez, F. Lloret, R. Carrasco, M. Julve, M. Verdaguer, Y. Dromzée, D. Gatteschi and W. Wernsdorfer, *Angew. Chem., Int. Ed.*, 2003, **42**, 1483; (d) S. Wang, J.-L. Zuo, S. Gao, Y. Song, H.-C. Zhou, Y.-Z. Zhang and X.-Z. You, *J. Am. Chem. Soc.*, 2004, **126**, 8900; (e) R. Lescouëzec, L. M. Toma, J. Vaissermann, M. Verdaguer, F. S. Delgado, C. Ruiz-Pérez, F. Lloret and M. Julve, *Coord. Chem. Rev.*, 2005, **249**, 2691; (f) L. M. Toma, R. Lescouëzec, J. Pasán, C. Ruiz-Pérez, J. Pasán, J. Vaissermann, J. Cano, R. Carrasco, W. Wernsdorfer, F. Lloret and M. Julve, *J. Am. Chem. Soc.*, 2006, **128**, 4842; (g) E. Coronado, J. R. Galán-Mascarós and C. Martí-Gastaldo, *J. Am. Chem. Soc.*, 2008, **130**, 14987; (h) L. Bogani, A. Vindigni, R. Sessoli and D. Gatteschi, *J. Mater. Chem.*, 2008, **18**, 4750; (i) H. Miyasaka, M. Julve, M. Yamashita and R. Clérac, *Inorg. Chem.*, 2009, **48**, 3420; (j) H. L. Sun, Z. M. Wang and S. Gao, *Coord. Chem. Rev.*, 2010, **254**, 1081; (k) T. D. Harris, M. V. Bennett, R. Clérac and J. R. Long, *J. Am. Chem. Soc.*, 2010, **132**, 3980; (l) X. Feng, T. D. Harris and J. R. Long, *Chem. Sci.*, 2011, **2**, 1688; (m) D. P. Dong, T. Liu, S. Kanegawa, S. Kang, O. Sato, C. He and C. Y. Duan, *Angew. Chem. Int. Ed.*, 2012, **51**, 5119; (n) L. M. Toma, J. Pasán, C. Ruiz-Pérez, F. Lloret and M. Julve, *Dalton Trans.*, 2012, **41**, 13716; (o) H. Miyasaka, T. Madanbashi, A. Saitoh, N. Motokawa, R. Ishikawa, M. Yamashita, S. Bahr, W. Wernsdorfer and R. Clérac, *Chem. Eur. J.*, 2012, **18**, 3942; (p) L. M. Toma, C. Ruiz-Pérez, J. Pasán, W. Wernsdorfer, F. Lloret and M. Julve, *J. Am. Chem. Soc.*, 2012, **134**, 15265.
- 24 R. J. Glauber, *J. Math. Physics*, 1963, **4**, 294.
- 25 (a) E. Pardo, C. Train, R. Lescouëzec, Y. Journaux, J. Pasán, C. Ruiz-Pérez, F. S. Delgado, R. Ruiz-García, F. Lloret and C. Paulsen, *Chem. Commun.*, 2010, **46**, 2322; (b) J. Ferrando-Soria, D. Cangussu, M. Eslava, Y. Journaux, R. Lescouëzec, M. Julve, F. Lloret, J. Pasán, C. Ruiz-Pérez, E. Lhotel, C. Paulsen and E. Pardo, *Chem. Eur. J.*, 2011, **17**, 12482.
- 26 T. Grancha, C. Tourbillon, J. Ferrando-Soria, M. Julve, F. Lloret, J. Pasán, C. Ruiz-Pérez, O. Fabelo and E. Pardo, *CrystEngComm*, 2013, **15**, 9312.
- 27 J. Ferrando-Soria, R. Ruiz-García, J. Cano, S.-E. Stiriba, J. Vallejo, I. Castro, M. Julve, F. Lloret, P. Amorós, J. Pasán, C. Ruiz-Pérez, Y. Journaux and E. Pardo, *Chem. Eur. J.*, 2012, **18**, 1608.
- 28 J. Ferrando-Soria, P. Serra-Crespo, M. de Lange, J. Gascon, F. Kapteijn, M. Julve, J. Cano, F. Lloret, J. Pasán, C. Ruiz-Pérez, Y. Journaux and E. Pardo, *J. Am. Chem. Soc.*, 2012, **134**, 15301.
- 29 J. Ferrando-Soria, H. Khajavi, P. Serra-Crespo, J. Gascon, F. Kapteijn, M. Julve, F. Lloret, J. Pasán, C. Ruiz-Pérez, Y. Journaux and E. Pardo, *Adv. Mater.*, 2012, **24**, 5625.
- 30 (a) R. E. P. Winpenney, *Adv. Inorg. Chem.*, 2001, **52**, 1; (b) D. Gatteschi and R. Sessoli, *Angew. Chem. Int. Ed.* 2003, **42**, 268; (c) L. Thomas, F. Lionti, R. Ballou, D. Gatteschi, R. Sessoli and B. Barbara, *Nature*, 1996, **383**, 145; (d) J. R. Friedman, M. P. Sarachik, J. Tejada and R. Ziolo, *Phys. Rev. Lett.*, 1996, **76**, 3830; (e) C. Coulon, R. Clérac, L. Lecren, W. Wernsdorfer and H. Miyasaka, *Phys. Rev. B*, 2004, **69**, 132408.
- 31 D. Gatteschi, R. Sessoli and J. Villain, *Molecular Nanomagnets*, Oxford University Press, 2006.
- 32 J. Crassous, *Chem. Commun.*, 2012, **48**, 9687.
- 33 G. L. J. A. Rikken and E. Raupach, *Nature*, 1997, **390**, 493.

- 34 (a) Hashimoto, *Angew. Chem. Int. Ed.*, 2007, **46**, 3238; (b) P. Jain, V. Ramachandran, R. J. Clark, H. D. Zhou, B. H. Toby, N. S. Dalal, H. W. Kroto and A. K. Cheetham, *J. Am. Chem. Soc.*, 2009, **131**, 13625; (c) G.-C. Xu, W. Zhang, X.-M. Ma, Y.-H. Chen, L. Zhang, H.-L. Cai, Z.-M. Wang, R.-G. Xiong and S. Gao, *J. Am. Chem. Soc.*, 2011, **133**, 14948; (d) A. O. Polyakov, A. H. Arkenbout, J. Baas, G. R. Blake, A. Meetsma, A. Caretta, P. H. M. Loosdrecht and T. T. M. Palstra, *Chem. Mater.*, 2012, **24**, 133.
- 35 (a) S. Bénard, P. Yu, J. P. Audiere, E. Riviere, R. Clément, J. Guilhem, L. Tchertanov and K. Nakatani, *J. Am. Chem. Soc.*, 2000, **122**, 9444; (b) J. S. O. Evans, S. Bénard, Y. Pei and R. Clément, *Chem. Mater.*, 2001, **13**, 3813; (c) M. Gruselle, B. Malézieux, S. Bénard, C. Train, C. Guyard-Duhayon, P. Gredin, K. Tonsuaadu and R. Clément, *Tetrahedron Assym.*, 2004, **15**, 3103; (d) E. Cariati, R. Macchi, D. Roberto, R. Ugo, S. Galli, N. Casati, P. Macchi, A. Sironi, L. Bogani, A. Caneschi and D. Gatteschi, *J. Am. Chem. Soc.*, 2007, **129**, 9410; (e) E. Cariati, R. Ugo, G. Santoro, E. Tordin, L. Sorace, A. Caneschi, A. Sironi, P. Macchi and N. Casati, *Inorg. Chem.*, 2010, **49**, 10894.
- 36 (a) O. Kahn, J. Larianova and J. V. Yakhmi, *Chem. Eur. J.*, 1999, **5**, 3443; (b) J. Larionova, S. A. Chavan, J. V. Yakhmi, A. Gulbrandsen Froystein, J. Sletten, C. Sourisseau and O. Kahn, *Inorg. Chem.*, 1997, **36**, 6374.
- 37 (a) S. Kitagawa, R. Kitaura and S.-I. Noro, *Angew. Chem. Int. Ed.*, 2004, **43**, 2334; (b) S. Kitagawa and K. Uemura, *Chem. Soc. Rev.*, 2005, **34**, 109; (c) S. Kitagawa and R. Matsuda, *Coord. Chem. Rev.*, 2007, **251**, 2490.
- 38 (a) G. Férey, C. Mellot-Draznieks, C. Serre and F. Millange, *Acc. Chem. Res.*, 2005, **38**, 217; (b) G. Férey, *Chem. Soc. Rev.*, 2008, **37**, 191; (c) G. Férey and C. Serre, *Chem. Soc. Rev.*, 2009, **38**, 130.
- 39 C. Serre, C. Mellot-Draznieks, S. Surblé, N. Audebrand, Y. Filinchuk and G. Férey, *Science*, 2007, **315**, 1828.
- 40 D. Maspoch, D. Ruiz-Molina, K. Wurst, N. Domingo, M. Cavallini, F. Biscarini, J. Tejada, C. Rovira and J. Veciana, *Nature Mater.*, 2003, **2**, 190.
- 41 N. W. Ockwig, O. Delgado-Friedrichs, M. O'Keeffe and O. M. Yaghi, *Acc. Chem. Res.*, 2005, **38**, 176.
- 42 (a) G. J. Halder, C. J. Kepert, B. Moubaraki, K. S. Murray and J. D. Cashion, *Science*, 2002, **29**, 1762; (b) M. Ohba, K. Yoneda, G. Agustí, M. C. Muñoz, A. B. Gaspar, J. A. Real, M. Yamasaki, H. Ando, Y. Nakao, S. Sasaki and S. Kitagawa, *Angew. Chem. Int. Ed.*, 2009, **48**, 4652.
- 43 (a) H.-L. Jiang, Y. Tatsu, Z.-H. Lu and Q. Xu, *J. Am. Chem. Soc.*, 2010, **132**, 5586; (b) Y. Takashima, V. M. Martínez, S. Furukawa, M. Kondo, S. Shimomura, H. Uehara, M. Nakahama, K. Sugimoto and S. Kitagawa, *Nat. Comms.*, 2011, **2**, 168.
- 44 (a) T. C. Chao, Y. T. Lin, C. Y. Yang, T. S. Hung, H. C. Chou, C. C. Wu and K. T. Wong, *Adv. Mater.*, 2005, **17**, 992; (b) X. Hu, J. Deng, J. P. Zhang, A. Lunev, Y. Bilenko, T. Katona, M. S. Shur, R. Gaska, M. Shatalov and A. Khan, *Phys. Status Solidi A*, 2006, **203**, 1815; (c) S. Mochizuki, S. Minami and F. Fujishiro, *J. Lumin.*, 2005, **112**, 267; (d) C. D. Müller, A. Falcou, N. Reckefuss, M. Rojahn, V. Wiederhirn, P. Rudati, H. Frohne, O. Nuyken, H. Becker and K. Meerholz, *Nature*, 2003, **421**, 829; (e) M. Q. Zhu, L. Zhu, J. J. Han, W. Wu, J. K. Hurst and A. D. Q. Li, *J. Am. Chem. Soc.*, 2006, **128**, 4303; (f) K. Binnemans, *Chem. Rev.*, 2009, **109**, 4283; (g) S. H. Hwang, C. N. Moorefield and G. R. Newkome, *Chem. Soc. Rev.*, 2008, **37**, 2543; (h) S. V. Eliseeva and J. C. G. Bunzli, *Chem. Soc. Rev.*, 2010, **39**, 189; (i) M. D. Allendorf, A. Schwartzberg, V. Stavila and A. A. Talin, *Chem. Eur. J.*, 2011, **17**, 11372.
- 45 (a) M. Alvaro, G. A. Facey, H. García, S. García and J. C. Scaiano, *J. Phys. Chem.*, 1996, **100**, 18173; (b) M. Alvaro, H. García, S. García, F. Márquez and J. C. Scaiano, *J. Phys. Chem. B*, 1997, **101**, 3043.
- 46 T. Grancha, J. Ferrando-Soria, J. Cano, F. Lloret, M. Julve, G. De Munno, D. Armentano and E. Pardo, *Chem. Commun.*, 2013, **49**, 5942.
- 47 I. Imaz, M. Rubio-Martinez, J. An, I. Solé-Font, N. L. Rosi and D. Maspoch, *Chem. Commun.*, 2011, **47**, 7287, and references therein.